kerja sama
jerman
DEUTSCHE ZUSAMMENARBEIT

Implemented by:

giz Deutsche Gesellschaft
für Internationale
Zussamenarbeit (GIZ) GmbH

In cooperation with:

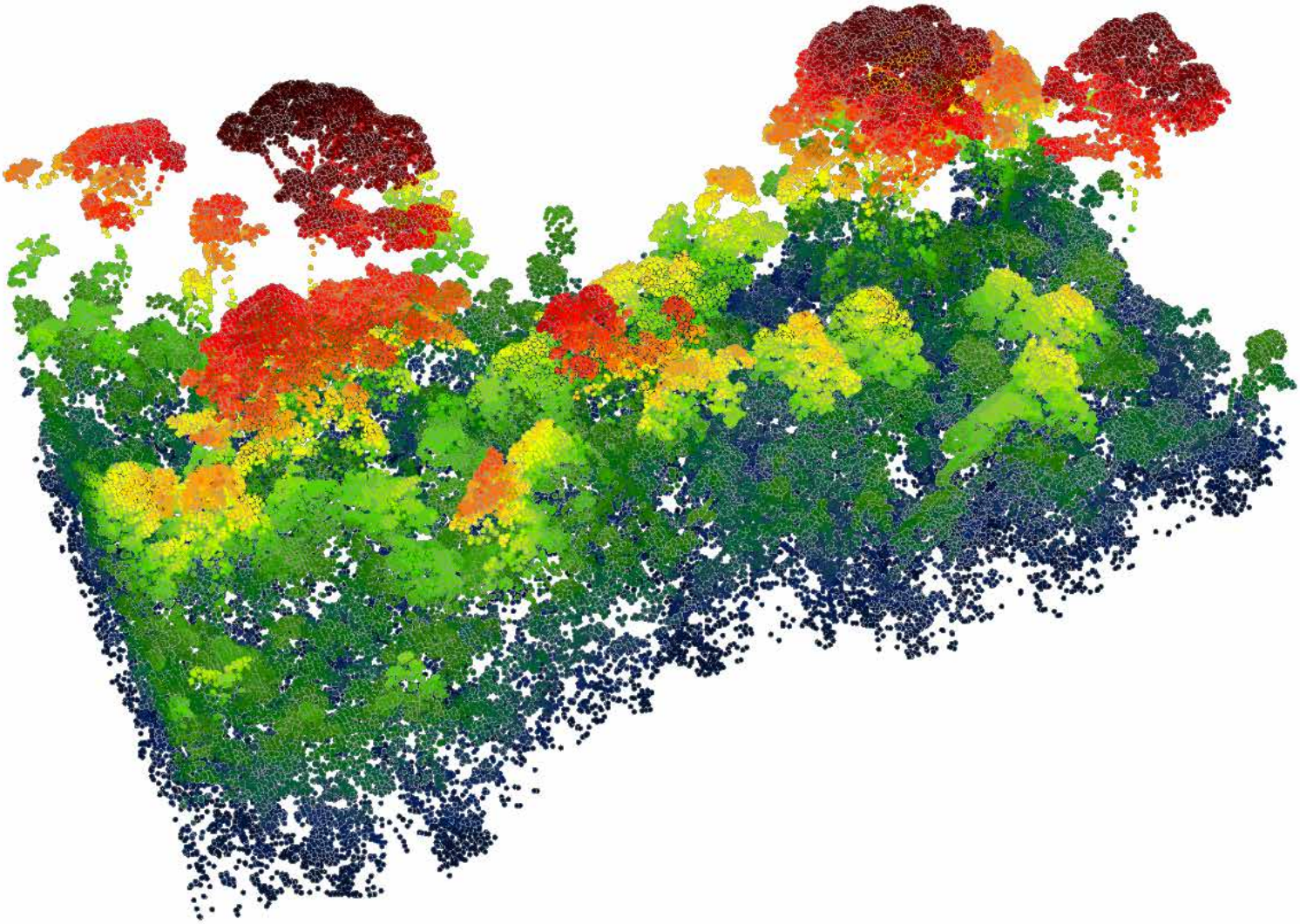

Development of LiDAR based aboveground biomass models in Kalimantan

Locally explicit emission factors in Kapuas Hulu, Berau and Malinau Districts

Published by:

Deutsche Gesellschaft für Internationale Zusammenarbeit (GIZ) GmbH
FORCLIME Forests and Climate Change Programme
Manggala Wanabakti Building, Block VII, 6th Floor Jln. Jenderal Gatot Subroto, Jakarta 10270, Indonesia
Tel: +62 (0)21 572 0212, +62 (0)21 572 0214
Fax: +62 (0)21 572 0193
www.forclime.org

In Cooperation with:

Ministry of Environment and Forestry

Authors:
Peter Navratil, Kristina Konecny, Juilson Jubanski, Uwe Ballhorn, Florian Siegert
RSS – Remote Sensing Solutions GmbH
Isarstraße 3
82065 Baierbrunn
Germany

Photo credits:

FORCLIME collection

Printed and distributed by:

FORCLIME

Jakarta, August 2016

Forests and Climate Change (FORCLIME)

FORCLIME Technical Cooperation (TC), a programme implemented by the Indonesian Ministry of Environment and Forestry and GIZ, and funded through the German Federal Ministry for Economic Cooperation and Development (BMZ)

Development of LiDAR based aboveground biomass models in Kalimantan

Locally explicit emission factors in Kapuas Hulu, Berau and Malinau Districts

Table of Contents

Appendix

Glossary

AGB	Above ground Biomass
BMZ	Bundesministerium fuer wirtschaftliche Zusammenarbeit und Entwicklung (German Federal Ministry for Economic Cooperation and Development)
CH	Centroid Height
CHM	Canopy Height Model
dbh	Diameter at Breast Height
DME	Distance Measuring Equipement
DSM	Digital Surface Model
DTM	Digital Terrain Model
FMU	Forest Management Unit
FORCLIME	Forests and Climate Change Programme
GCP	Ground Control Point
GIZ	Deutsche Gesellschaft fuer Internationale Zusammenarbeit (GIZ) GmbH
GPS	Global Positioning System
LiDAR	Light Detection And Ranging
PPR	Predictive Power of Regression
QMCH	Quadratic Mean Canopy Height
RMSE	Root Mean Squared Error
RSS	Remote Sensing Solutions GmbH
SD	Standard Deviation
SRTM	Shuttle Radar Topography Mission

Preface

The Technical Cooperation of Forests and Climate Change Program (FORCLIME TC) is a programme implemented by the Indonesian Ministry of Environment and Forestry and Deutsche Gesellschaft für Internationale Zusammenarbeit (GIZ), and funded through the German Federal Ministry for Economic Cooperation and Development (BMZ).

The programme's overall objective is to reduce greenhouse gas emissions from the forest sector while improving the livelihoods of Indonesia's poor rural communities. To achieve this goal, the programme team will assist the Indonesian government to design and implement legal, policy and institutional reforms for the conservation and sustainable management of forests, at local, provincial and national level. Support to REDD+ (Reducing Emissions from Deforestation and forest Degradation) demonstration activities is a key feature of the programme, providing decision-makers with experience of how REDD+ can be implemented "on the ground".

A forest reference emission level (FREL) is a benchmark for assessing a country's or region's performance in implementing *REDD+* activities. FORCLIME supports three districts in Kalimantan in developing their FREL and promotes to follow the national approach as close as possible and reasonable. Due to reasons of sustainability of availability of land cover data, using the national land cover data provided by MoEF is recommend. On the other hand, it is reasonable to develop locally explicit emission factors for each district because the specific composition of forest ecosystems and hence the carbon stock can vary quite significantly in different regions, even though they are categorized as the same forest type in the national system.

Therefore, FORCLIME has developed locally explicit emission factors for above ground biomass (AGB) based on data captured with Light Detection And Ranging (LiDAR) sensors in three districts in Kalimantan: Kapuas Hulu (West Kalimantan), Berau (East Kalimantan) and Malinau (North Kalimantan). This report describes in detail the acquisition of the LiDAR data and the development of the LiDAR biomass models.

Jakarta, August 2016

Georg Buchholz
FORCLIME Programme Director

1 Introduction

This report presents the results of an airborne LiDAR survey commissioned by the Indonesian-German Forests and Climate Change Programme (FORCLIME). The survey was carried out from September 2012 – September 2013, and covered three study areas in Kalimantan for which LiDAR data and digital aerial photos were acquired. The study areas comprise the Forest Management Units (FMU) in the three FORCLIME districts Kapuas Hulu, Berau and Malinau.

RSS – Remote Sensing Solutions GmbH (further referred to as RSS) was the main contractor and responsible for the project management, implementation and data analysis. Credent Technology Pty Ltd was subcontracted for the execution of the LiDAR and aerial photo data acquisition.

The key objective of the study was to establish an above ground biomass and carbon model for each "FORCLIME district" based on LiDAR technology that can be used to derive more accurate emission factors for a MRV system to quantify future biomass and carbon changes within the newly established Forest Management Units (FMU) in the three districts of Kapuas Hulu, Berau and Malinau, and to offer a concept that can be adapted at province and national scale.

In order to fulfill this objective, the following activities had to be carried out:

- Acquire LiDAR data for the three FMUs in the three districts.
- Process LiDAR data into Digital Surface Models (DSM), Digital Terrain Models (DTM) and Canopy Height Models (CHM).
- Develop LiDAR based biomass models for each of the districts based on sample plots from ongoing forest inventories (Kapuas Hulu, Malinau) and additional inventories (Berau), and then apply these models to the LiDAR transects.
- Acquire Rapid Eye data for the FMU area of Berau.
- Land cover classification for the Berau FMU based on the RapidEye data
- Derive local above ground biomass and carbon values and emission factors for the different forest ecosystems and degradation levels in the FMUs.
- Train local stakeholders in RapidEye interpretation and classification for land cover mapping

2 Data and methods

2.1 LiDAR survey

2.1.1 Survey specifications

The objective of the survey is to capture transects of LiDAR data and aerial photography with a width of 500 m. The target area in each district is approximately 25,000 ha.
Since the survey was started at the beginning of the rainy season 2012 in Kalimantan, one of the challenges was frequent cloud cover. Experience shown that the condensation level at this time of the year where clouds begin to form is around 900 m a.s.l.
In order to make sure that the LiDAR data capture remains free of clouds, it was decided to conduct the survey at an altitude of approximately 720 - 800 m above ground, in order for the airplane to stay below the clouds at all times. This flight altitude allows a transect width of the LiDAR data with two overflights of approx. 507 – 563 m with 35 % overlap of the two flight strips (see Figure 1).

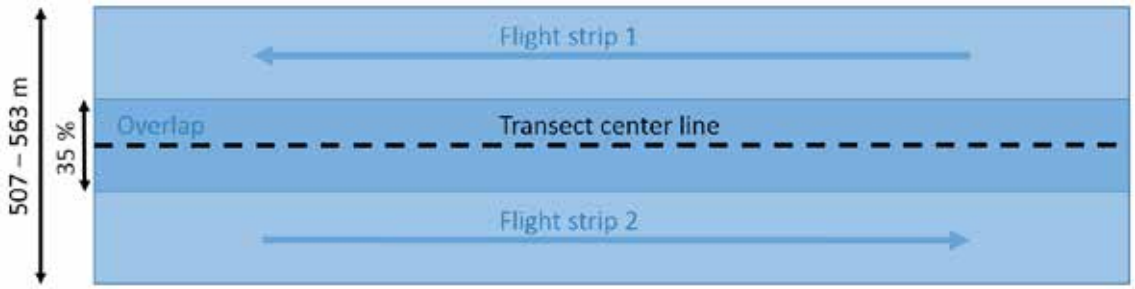

Figure 1: Flight planning for capturing 500 m wide transects from an altitude of 720 - 800 m above ground.

The technical specifications of the LiDAR data and aerial photos are listed below:

Vertical accuracy:	0.15m RMSE
Horizontal accuracy:	0.25m
Vertical datum:	EGM08
Projection:	Kapuas Hulu: UTM49N Berau: UTM50N Malinau UTM50N
Acquisition mode:	Discrete return
LiDAR scanner:	Optech ALTM 3100
Half-scan-angle:	max. 12°
Point density:	3-5 pts/ m²
Ground sampling density Aerial photography:	10-20cm

2.2 LiDAR data processing

2.2.1 Filtering and interpolation

The first step is the filtering of the LiDAR point clouds. This is an essential step, since the DTMs are directly derived from the filtered point clouds. In this study, the filtering is the separation between ground and off-ground LiDAR points, since within the study area nearly all off-ground points consist of vegetation, no further classification is necessary.

Both filtering and interpolation solutions used by RSS are implemented within the Inpho software package (DTMaster and SCOP++). This package was chosen due to its high computational performance, reliability, and extensive documentation.

The filtering methodology used is the Hierarchic Robust Filtering (Pfeifer *et al.* 2001). This works in a coarse to fine strategy, adding more terrain detail in each step. This method is comparable to a hierarchical setup using image pyramids. The structure of the pyramids is regular, as typically done with images, and the reduction function operates directly in the point cloud. The methodology consists of three steps:

Step 1: Creation of data pyramids.

Step 2: The Robust Filtering and the DTM generation itself.

Step 3: Comparison of the DTM to data with higher resolution and iterative addition of points for generating the terrain model.

The Hierarchical Robust Filtering algorithm is based on linear prediction with individual accuracies for each measurement and works iteratively. In the first step, all points are used to estimate the covariance function of the terrain. The first surface is computed with equal weights for all points and runs in an averaging way between ground and vegetation points. Ground points are more likely to:

- be below the averaging surface,
- have negative filter values,
- have positive residuals.

Vegetation points tend to:

- be above or on the averaging surface,
- have positive filter values,
- have negative residuals.

After the first model deviation, the filter values are computed and the weight of the points is altered according to the weight function. If a point is given a low weight, it will have lower influence on the run of the surface in the next iteration.

Two methods are used in order to determine the surface:

- Prediction: It is a flexible method in the sense that it computes a surface that approximates the given data. The flexibility is controlled by a covariance function which is determined from the data.
- Trend: This method computes a plane for each computing unit. A plane is very inflexible and this method is good for removal of gross errors.

The implementation methodology runs iteratively a trend surface followed by prediction, so that initially gross errors are eliminated before a refined filter is run. Although all parameters can be freely chosen, the methodology as a whole is called robust because it is quite independent of input parameters for the weighting functions. The results of the filtering operation were visually inspected and remaining outliers were removed interactively.

Terrain surfaces are an idealization and an abstraction of the Earth's surface. They tend to be smooth with continuous differentials over large areas. They may be area type structures as well as linear structures. Furthermore, one has to differentiate between large forms and small forms. Larger forms represent the terrain surface on a large scale, while small forms are local departures of the general surface. Discontinuities exist in the form of surface edges and escarpments, where surface edges are discontinuities of the first differential and escarpments are discontinuities of the functional values themselves. These discontinuities do not directly exist on the Earth's surface, but they are generated by scaling down the surface and the projection of the surface onto the horizontal plane.

For the precise description of the terrain surface, SCOP++ uses linear prediction. The theoretical basis of linear prediction is presented in detail in various scientific publications (Kraus 1998; Assmus 1975; Wild 1983). Linear adaptable prediction corresponds to the statistical estimation method Kriege, often applied in Geo-sciences (Kraus 1998). Figure 2 shows the mathematical principle of this filtering algorithm. The idea is to iteratively run the algorithm for each processing unit (cells) until all points within this cell has a final height of 1 (ground) or 0 (not-ground). We processed the data with a cell size of 3 m.

$$p_i = \begin{cases} 1 & f_i \leq g \\ \dfrac{1}{1+(a(f_i-g))^b} & g < f_i \leq t \\ 0 & t < f_i \end{cases}$$

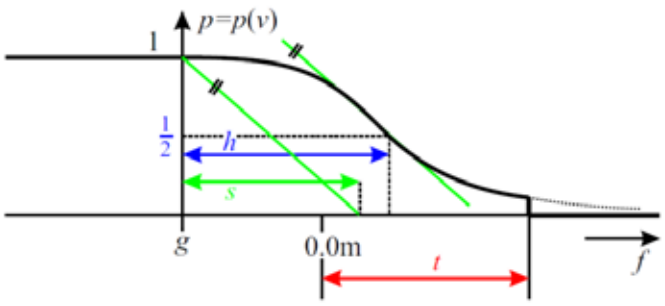

Source: Pfeifer et al. 2001

Figure 2: Mathematical principle of the filtering algorithm

2.3 Orthophoto production and Mosaicking

Ortho photos do not contain the scale, tilt, and relief distortions characterizing aerial photos. To produce ortho photos from digital aerial photos a DTM is needed. The aerial photos were re-projected orthographically using the elevation information from the LiDAR DTM and orientation parameters (obtained by GNSS and IMU systems) to remove these effects.

2.4 Field inventory data

Forest inventories were planned by FORCLIME in each of the districts in order to collect calibration data for the establishment of LiDAR based above ground biomass models.The sampling was conducted along the centerline of the LiDAR transects in order to maximize the usability of the field data for calibrating the LiDAR models. A random sampling strategy was applied to determine the exact plot location along the transect. The inventory data from both districts have a very high quality.

In Berau and Kapuas Hulu the sample plots were fixed in area and circular in shape consisting of nested subplots arranged in concentric circles (see Figure 3). Nested sample plots are recommended in highly diverse tropical forests in order to get information on both widly distributed large trees and also on smaller but more densely distributed trees. In comparison to rectangular plots circular plots have the advantage that they are less vulnerable to errors of trees located on the plot boundary, since the perimeter is smaller in relation to the area compared to that of a rectangular plot. Additionally circular plots are easy to install using Distance Measuring Equipment (DME), because the boundary of the plot does not need to be marked (Lackmann 2011). Finally for rectangular plots a slope correction is difficult to calculate, especially if the slope is oriented to more than one direction on the sample plot.

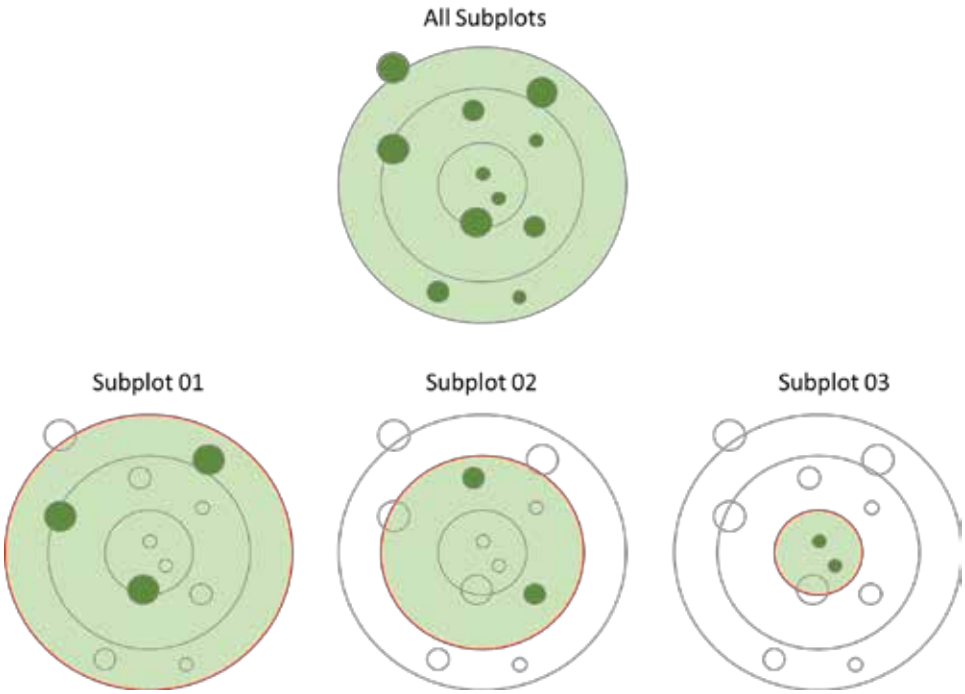

Figure 3: Example of a nested plot consisting of three subplots. In each of these subplots trees with different diameter at breast height (dbh) are measured.

Table 1 gives a detailed description of the forest inventories in Berau and Kapuas Hulu.

Table 1: Detailed describtion of the forest inventories in Berau and Kapuas Hulu.

Berau	Kapuas Hulu
Plot Design	
79 plots with following plot design were recorded: ▪ Subplot 01: diameter at breast height (dbh) ≥50 cm; 35 m radius (horizontal distance; area = 3,848.45 m^2); to calibrate the LiDAR data a 30 m radius was applied (trees with a distance of more than 30 m were excluded; area = 2,827.43 m^2) ▪ Subplot 02: dbh ≥20 cm and <50 cm; 25 m radius (horizontal distance); area = 1,963,50 m^2 ▪ Subplot 03: dbh ≥10 cm and <20 cm; 10m radius (slope distance); area = 314,16 m^2; slope correction ▪ Subplot 04: dbh ≥2 cm and <10 cm; 3 m radius (slops distance); area = 28,27 m^2; slope correction	44 plots with following plot design were recorded: ▪ Subplot 01: diameter at breast height (dbh) ≥50 cm; 30 m radius (slope distance); area = 2,827.43 m^2 ▪ Subplot 02: dbh ≥20 cm and <50 cm; 20 m radius (slope distance); area = 1,256,64 m^2 ▪ Subplot 03: dbh ≥10 cm and <20 cm; 10 m radius (slope distance); area = 314,16 m^2; slope correction ▪ Subplot 04: dbh ≥2 cm and <10 cm; 3 m radius (slops distance); area = 28,27 m^2; slope correction
Parameters sampled in the Field	
▪ GPS coordinates ▪ Tree azimuth and distance from plot center for each tree ▪ Tree species ▪ Diameter at Breat Height (dbh, 1.30 m) ▪ Tree height: for 1-2 large trees with dbh>40 cm ▪ Crown class: for each tree, 1- emergent trees, 2- regular canopy trees, 3- regular canopy trees with slim canopy, 4- upper layer understory trees, 5- lower layer understory trees ▪ Damage class: for each tree, 0- no damage, 1- severe crown damage, 2-severe trunk damage, 3- severe crown and trunk damage ▪ Slope (%): measured for each individual tree in subplot 01 and 02	▪ GPS coordinates ▪ Tree azimuth and distance from plot center for each tree ▪ Tree species ▪ Diameter at Breat Height (dbh, 1.30 m) ▪ Tree height: average tree height for the trees in subplots 01 and 02 ▪ Damage class: for each tree, 0- no damage, 1- severe crown damage, 2-severe trunk damage, 3- severe crown and trunk damage ▪ Slope (%): avarege for the measured for subplots 01 and 02
Wood Density	
For all species with scientific names, wood density values were obtained from the Global Density Database (Zanne et al. 2009). For species unknown, an average wood density of 0.57 t/m^3 for Asian tropical forests was applied (Brown 1997).	For all species an average wood density of 0.57 t/m^3 for Asian tropical forests was applied (Brown 1997).

Table 1: (Continued)

Berau	Kapuas Hulu
Above Ground Biomass (AGB)	
The AGB was estimated for each tree using an generic allometric equation for tropical moist forest stands excluding tree height (Chave et al. 2005) $AGB = \rho \times \exp(-1.499 + 2.148 \ln(D) + 0.207 (\ln(D))^2 - 0.0281 (\ln(D))^3)$ Where: ρ = wood density D = diameter at breast height (dbh) The AGB estimations for the single trees were then extrapolated to estimates for one hectare.	
For species were the wood density was not known, an average wood density of 0.57 t/m^3 for Asian tropical forests was used (Brown 1997).	An average wood density of 0.57 t/m^3 for Asian tropical forests was used (Brown 1997)
Sample Area Slope correction	
The horizontal tree distance ($Dist_h$) of all trees in subplot 1 and 2 was calculated using following formula: $Dist_h = \cos(\tan\text{-}1(\text{slope }\%)) + Dist_h$ Mathematical plot area reduction for subplots 03 and 04 was carried out applying the same formula but using the average slope % of the sample plot. For the calculation of the average slope, the sample plot was subdivided into 12 segments of 30°, and the average slope calculated from the slope values of alltrees in that segment. Afterwards, the average segment slope values were averaged.	Mathematical plot area reduction for subplots 01 and 02 was carried out applying following formula: $Dist_h = \cos(\tan\text{-}1(\text{slope }\%)) + Dist_h$
Plot Position Correction	
With the GPS device plot tracks were recorded in order to improve accuracy beneath canopy cover. An average mid-point needed to be extracted from these tracks. This was done with the help of a standard ArcGIS function (Feature to Point) that first weights the vertex points according to the length of the line connecting them and then calculates the average coordinate over all of the weighted vertex points. This way the average GPS accuracy could be improved to about 3-4 m.	No plot position correction of the GPS data was carried out.

2.5 Approach for LiDAR based Above ground Biomass Models

Previous studies revealed that height metrics like the Quadratic Mean Canopy Height (QMCH) or the Centroid Height (CH) are appropriate parameters of the LiDAR point cloud to estimate AGB in tropical forests by taking also the point distribution over the different vegetation layers into account (Ballhorn *et al.* 2011; Jubanski *et al.* 2012; Kronseder *et al.* 2012). LiDAR height histograms were calculated by normalising all points within a grid of 30 m (similar to the size of the largest nest of the field inventory plots) to the ground using the DTM as reference. A height interval of 0.5 m was defined and the number of points within this interval was stored in form of a histogram. The first (lowest) interval was considered as ground return and therefore excluded from further processing.

The QMCH and the CH of the height histogram were calculated by weighing each 0.5 m height interval with the relative number of LiDAR points stored within this interval. QMCH and CH were related to field inventory estimated AGB and regression models were developed. Jubanski et al. (2012) showed that the accuracy of AGB estimations derived from LiDAR height histograms increased with higher point densities. For this reason, point density was also implemented in the regression as a weighting factor.
The commonly used power functions resulted in significant overestimations in the higher biomass range within our study areas (Asner et al. 2012; Jubanski et al. 2012). For this reason, a more appropriate AGB regression model was developed, which is a combination of a power function (in the lower biomass range up to certain threshold QMCH0; the example here uses QMCH but the same would be done with CH) and a linear function (in the higher biomass range). The threshold of QMCH0 was determined by increasing the value of QMCH0 in steps of 0.001 m through identifying the lowest RMSE. The linear function is the tangent through QMCH0 and was calculated on the basis of the first derivative of the power function:

$$AGB = \begin{cases} a \cdot QMCH^{b} & if\ QMCH \leq QMCH_0 \\ \left(a \cdot b \cdot QMCH_0^{(b-1)}\right)(QMCH - QMCH_0) + a \cdot QMCH_0^{b} & if\ QMCH > QMCH_0 \end{cases}$$

where QMCH is the Quadratic Mean Canopy Height (the example here uses QMCH but the same would be done with CH), QMCH0 is the threshold of function change and a, b are coefficients.

Next the AGB regression model with the best coefficient of determination (r2) based on the QMCH or the QMCH was then chosen. This AGB regression model was then independently validated by the Predictive Power of the Regression (PPR) as demonstrated by Asner et al. (2010). The PPR determines the RMSE by running 1,000 iterations of the regression and randomly leaving out 10 % of reference field inventory plots.

2.6 RapidEye image procurement and processing

2.6.1 Data procurement

RapidEye satellite images were procured for a complete coverage of the Forest Management Unit (FMU). Since there were no archived images available for the area of interest at project start, the acquisition of new imagery was tasked for wall-to-wall coverage. Due to persistent cloud cover of the FMU, it was necessary to keep the tasking up for the period September 2012 until August 2014. Seven RapidEye scenes were acquired in total until a complete coverage was achieved. The images procured are listed in Table 2.

Table 2: RapidEye satellite images procured for this study.

Image ID	Acquisition date
2012-09-18T033207_RE5_1B-NAC_10972461_148654	18.09.2012
2013-01-08T034159_RE2_1B-NAC_11494634_151250	08.01.2013
2013-05-14T032855_RE5_1B-NAC_15436566_177074	14.05.2013
2013-06-08T033515_RE1_1B-NAC_12962547_163418	08.06.2013
2013-06-19T034538_RE2_1B-NAC_13059496_163418	19.06.2013
2014-02-06T033450_RE1_1B-NAC_15431451_175807	06.02.2014
2014-05-18T033517_RE2_1B-NAC_16407849_179792	18.05.2014

2.6.1 Preprocessing

2.6.1.1 Geometric correction

The first processing step was the geometric correction of the satellite images so that they overlay correctly with other satellite data available in the project (in particular the Landsat imagery used in the REL study and the produced maps). The geometric correction was done by GCPs generated in a semi-automatic image-to-image matching procedure (Autosync) based on the Landsat image mosaics. Rectification was performed by the GCPs and the orientation parameters of the RapidEye images, and a terrain correction (ortho-rectification) was performed by the use of a digital elevation model (SRTM-90).

Table 3 lists the results of the geometric correction of the data. The images were resampled into the target UTM system (Zone 50N) with bilinear resampling.

Table 3: Results of the geometric correction

Image acquisition date	RMSE	Number of GCPs
18.09.2012	2.43	133
08.01.2013	2.32	256
08.06.2013	0.59	2,991
19.06.2013	0.95	259
06.02.2014	0.57	1,632
14.05.2013	1.58	532
18.05.2014	5.44	139

2.6.1.2 Atmospheric correction

Atmospheric correction was performed on the images in order to correct for differences in illumination situation between the image acquisitions, remove athmospheric distortions in the images (e.g. due to water vapour, haze) and to calibrate the imagery into an estimation of the surface reflectance. The correction was done by the software ATCOR-2 (Richter & Schläpfer 2014) which makes use of the MODTRAN atmospheric transfer model.

2.6.2 Land cover classification

The land cover classification was done with the Software eCognition which uses an object based image classification method. The first step of the classification process is the image segmentation, which accumulates spatially adjacent pixels with similar spectral properties into image objects. A threshold-based classification rule-set was then used to assign the land cover classes shown in Table 4 to the image objects. Eventually, a visual screening of the classification results was conducted in order to reduce mis-classifications and improve classification accuracy. The classification scheme is based on the same classes that were used for the forest benchmark mapping already conducted in Kapuas Hulu and Malinau, in order to facilitate maximum comparability.

Table 4: Classification scheme used for the RapidEye classification. Classes marked in bold are newly introduced in comparison to the historic land cover maps of Berau.

Classification Level 1	**Classification level 2**	**Classification level 3**
Forest	Type	Disturbance status*
	Lowland Dipterocarp Forest (0 - 300m a.s.l.)	Primary
		Secondary
	Hill and sub-montane Dipterocarp Forest (300-900m a.s.l.)	Primary
		Secondary
	Lower Montane Rain Forest (900 - 1500m a.s.l.)	Primary
		Secondary
	Upper Montane Rain Forest (> 1500m a.s.l.)	Primary
		Secondary
	Peat Swamp Forest	Primary
		Secondary
		Low Pole Peat Swamp Forest
	Heath Forest	Primary
		Secondary
	Riparian Forest (incl. Small holder rubber plantation)	Primary
		Secondary
	Freshwater Swamp Forest	Primary
		Secondary

Table 4: (Continued)

Classification Level 1	Classification level 2	Classification level 3
Non-forest	Plantation	
	Shrubs, Shifting cultivation, Smallholder agriculture, Grassland	
	Settlement	
	Wetland	
	Rice paddy	
	Bare Area	
	Water	

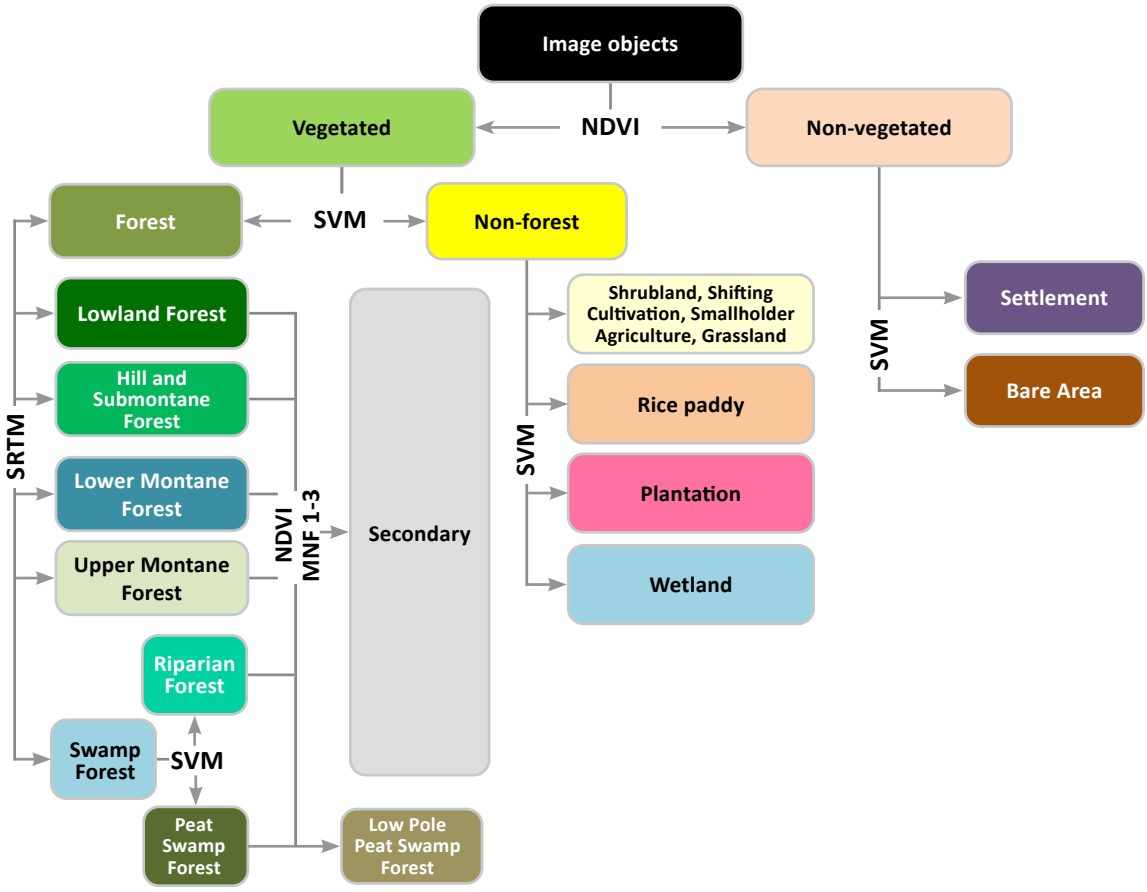

Figure 4: Structure of the classification ruleset for the RapidEye images.

2.6.3 Accuracy assessment

An accuracy assessment was conducted based on the forest inventory data collected by the FORCLIME programme, as well as the ground truth data collected in the Berau FMU in 2011 and 2012. The accuracy assessment utilized confusion matrices to derive overall map accuracy as well as class-wise producer's and user's accuracy.

2.7 Derive local AGB values for the different land cover categories

The resulting LiDAR AGB model and the land cover classification were overaid in order to extract local AGB values for the different land cover types from the AGB model. Within the class boundaries, a set of random sample points were generated for each class, and the AGB value and the land cover type was extracted into the attribute table at each point. The amount of sample points was based on the spatial extent of the classes, applying a sampling density of 20 points per ha with at least 5m spacing between the points. Furhter, the points were sampled only within a distance of more than 30 meters from the class boundaries in order to avoid errors in the class assignment due to geolocation errors. Then the descriptive statistics Minimum, Maximum, Average, Standard deviation and Variance, as well as the interval of confidence of the mean were calculated for each class. The results of this analysis, as well as the amount of sample points per class are shown in Table 8 and Table 9 in the results chapter 3.5.

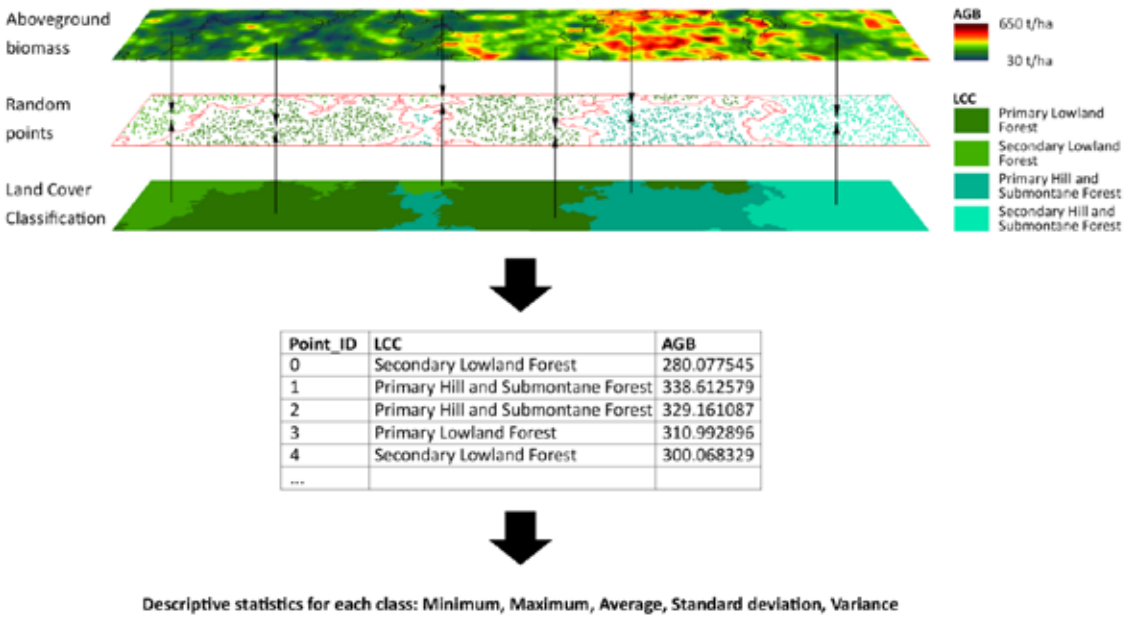

Figure 5: Intersection of the LiDAR AGB model with the land cover map. Random sample points were created within each land cover class and the AGB value extracted from the model at each point location. Finally, descriptive statistics were calculated for each land cover class.

3 Results

3.1 LiDAR and Orthophoto data

3.1.1 Coverage in each district, point density, orthophotos etc.

Table 5: Spatial extent and average point density of the LiDAR datasets collected in each district.

	LiDAR coverage [ha]	Average point density [points/m²]
Berau	33,671	7.0
Malinau	23,842	7.3
Kapuas Hulu	41,384	6.4
Total	**98,897**	**6.8**

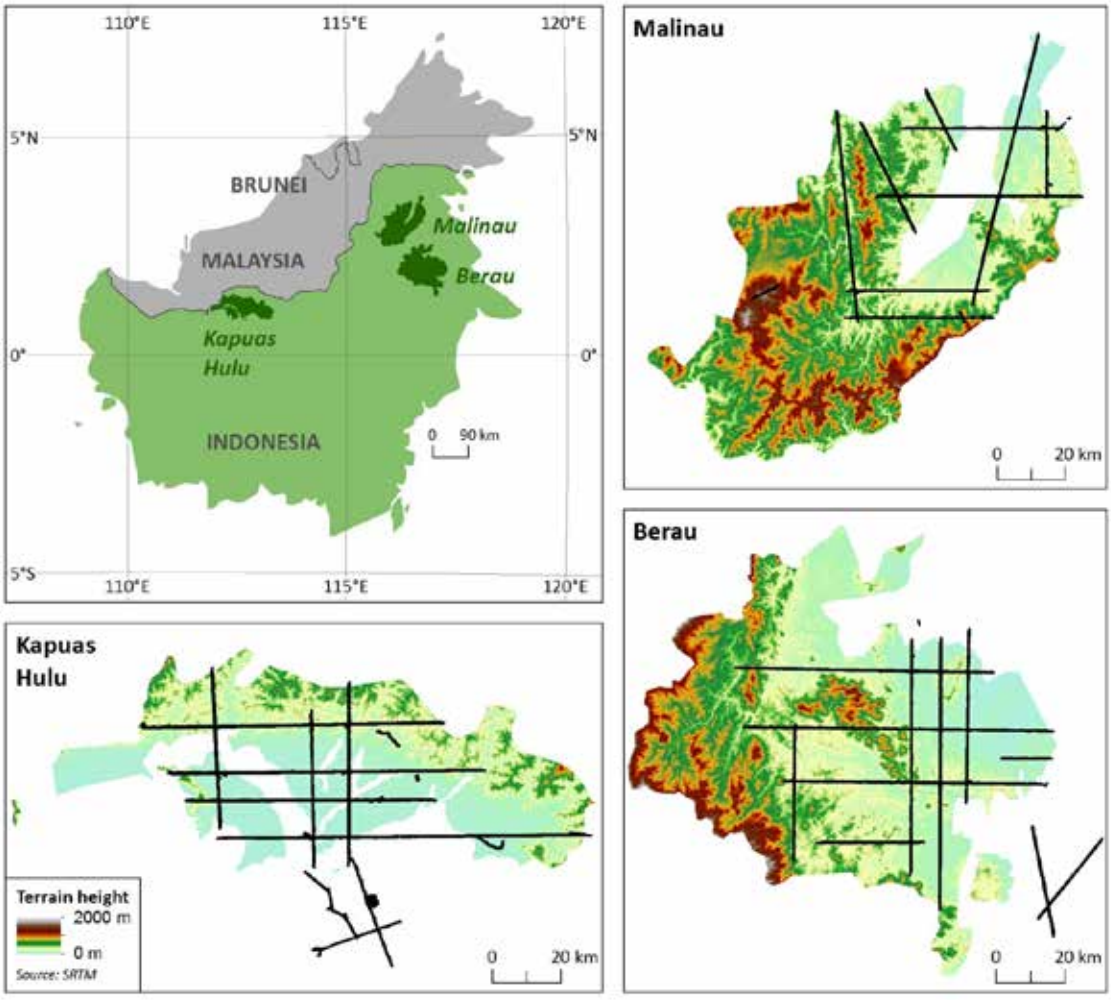

All LiDAR transects were also covered by digital orthophotos. The orthophotos were processed based on the interior and exterior orientation parameters and a terrain correction was applied using the LiDAR Digital Surface Model. The photos were then resampled to 25 cm GSD and mosaicked into image strips for each transect.

3.1.2 LiDAR products

For each of the study areas three basic LiDAR products were derived: A digital surface model (DSM), a digital terrain model (DTM) and a canopy height model (CHM).

The models were produced at a spatial resolution of 1 m and a vertical resolution of 1 cm. As the resulting raster datasets have a considerable file size, the data was split into tiles. Figure 6, Figure 7 and Figure 8 shows the resulting models for the three study areas.

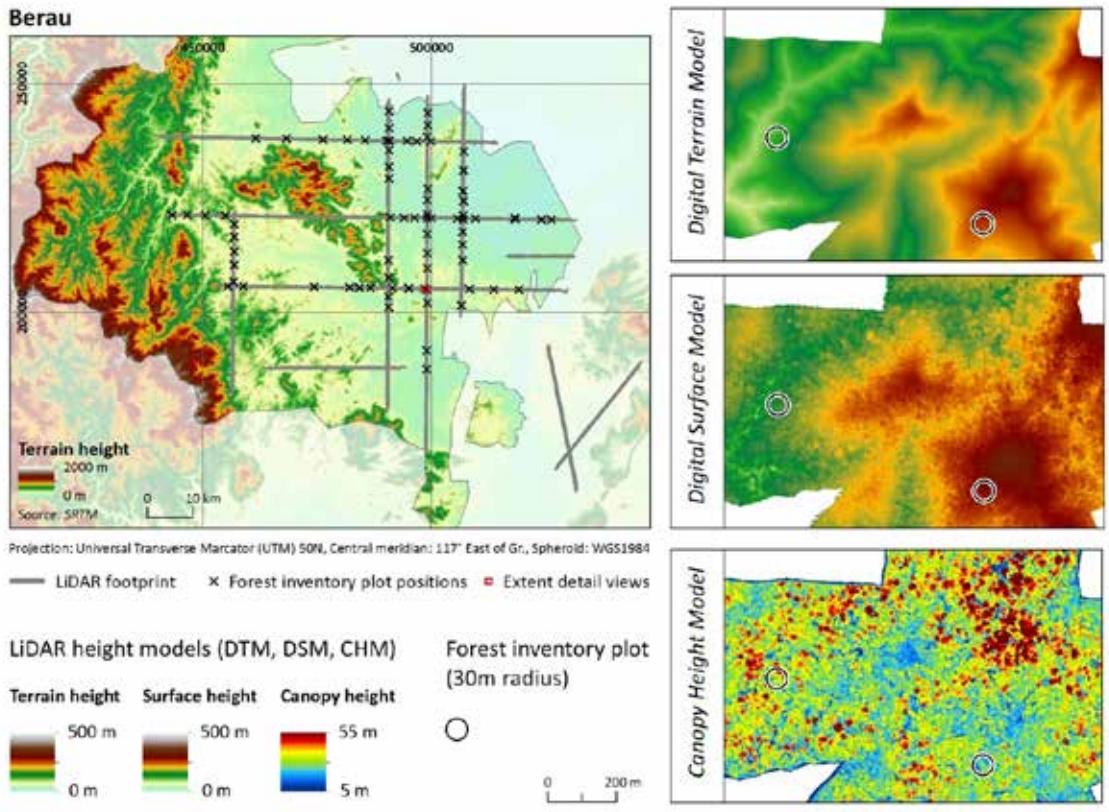

Figure 6: Example from the LiDAR products generated for Berau. Also shown are the positions of the 79 forest inventory plots.

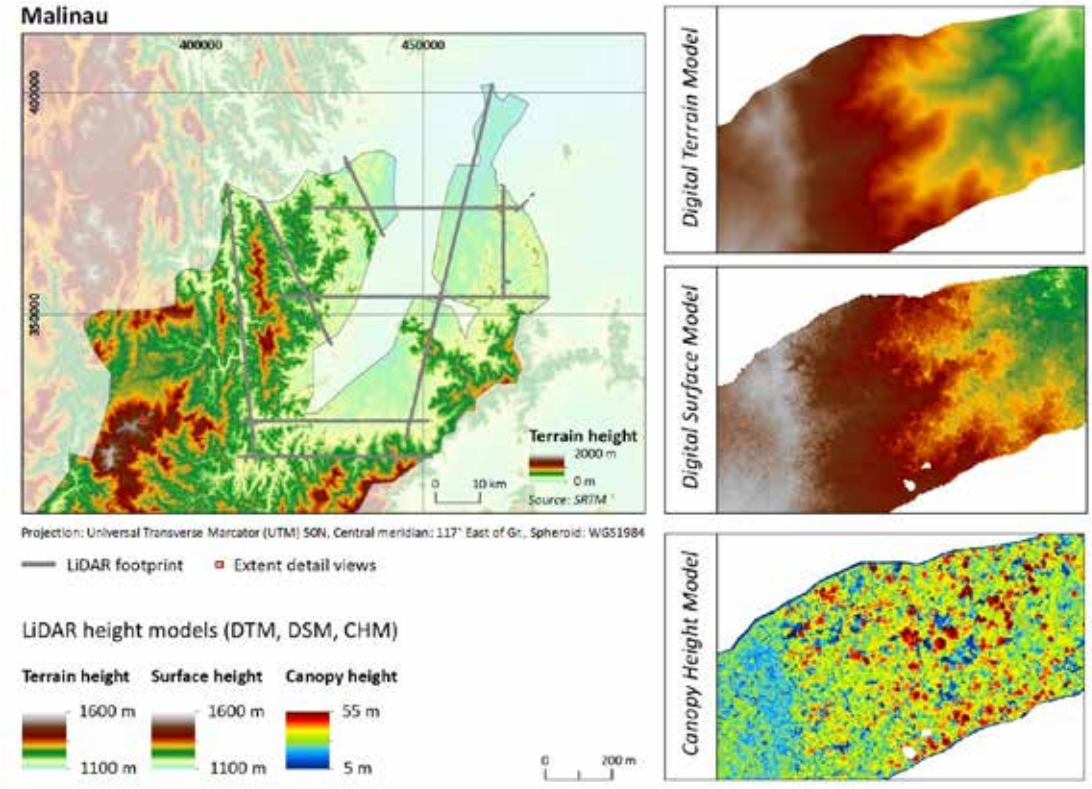

Figure 7: Example from the LiDAR products generated for Malinau.

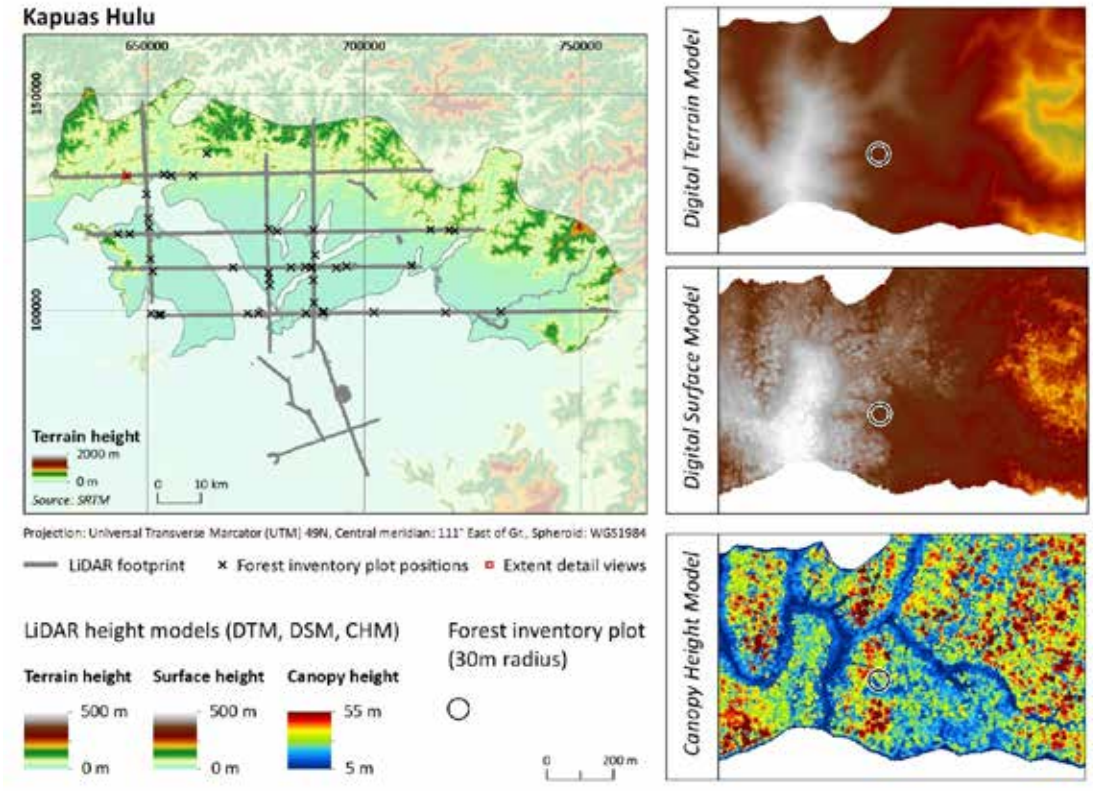

Figure 8: Example from the LiDAR products generated for Kapuas Hulu. Also shown are the positions of the 44 forest inventory plots.

3.1.3 LiDAR point clouds

The LiDAR point clouds were filtered as described in chapter 2.2.1 and then classified into ground and off-ground points. Again, for ease of handling, the classified point clouds are delivered in tiles.

Figure 9 shows some example sections representing different forest types and degradation stages in the LiDAR point clouds.

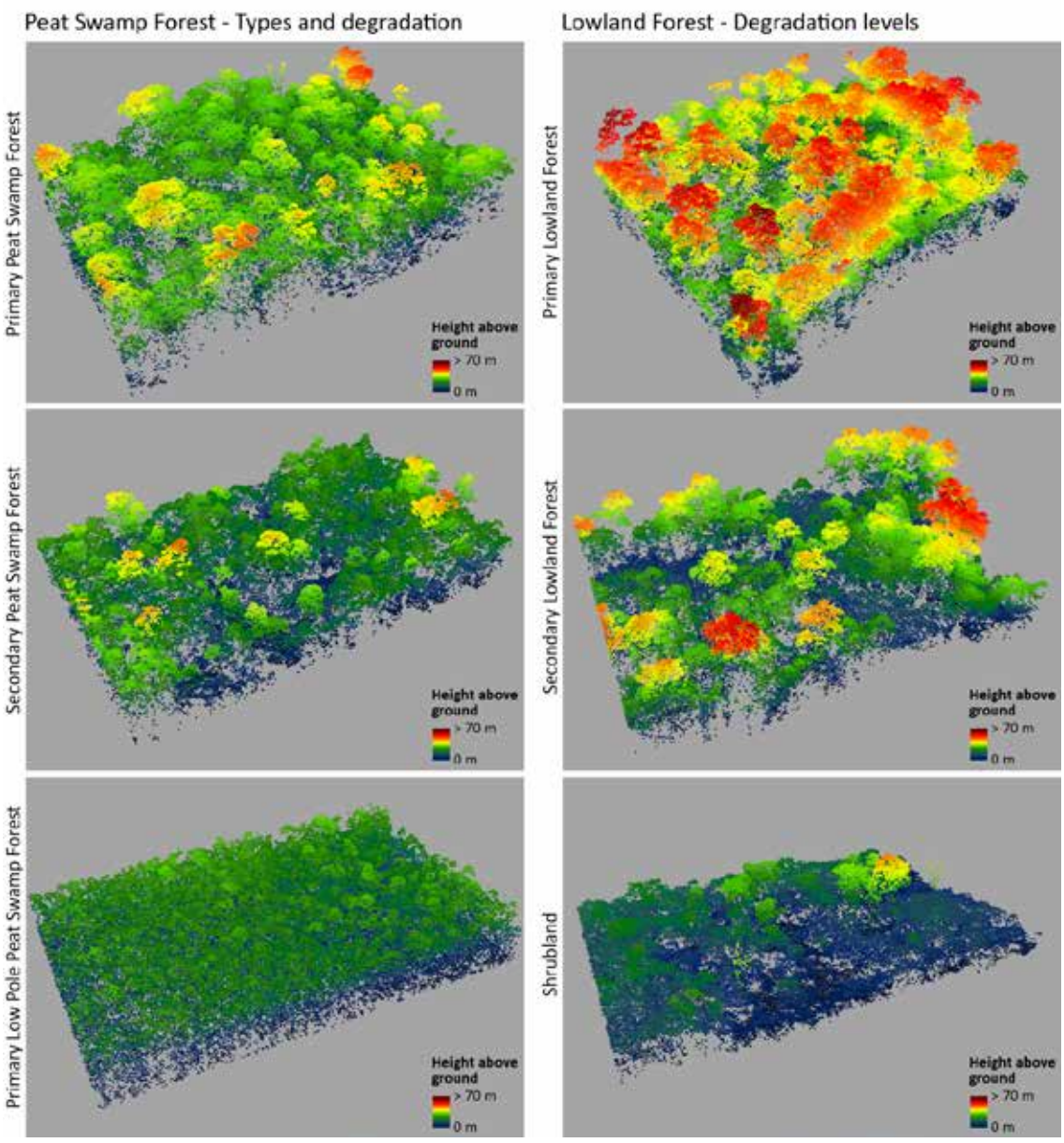

Figure 9: Examples of different forest types as seen in the LiDAR point cloud.

3.2 Field inventory data used for AGB prediction models

The location of the nested field plots for Berau (79 plots) and Kapuas Hulu (44 plot) are shown in Figure 6 and Figure 8. Table 6 additionally displays the main statistics considering AGB estimates from these two forest inventories. This table shows that the average AGB estimate per hectare was about 15 tons higher in Kapuas Hulu than in Berau. Also, the maximum AGB estimate with 900.10 tons was about 156 tons higher than in Berau. These two numbers might indicate a higher biomass occurrence in Kapuas Hulu. The higher standard deviation and confidence interval on the other hand also suggest that the AGB variability might be higher in Kapuas Hulu.

As the field inventory is still ongoing, no information can be given for the sample plots within Malinau district.

Table 6: Main statistics considering Above Ground Biomass (AGB) estimates from the two forest inventories in Berau and Kapuas Hulu (in Kapuas Hulu three inventory plot were excluded because at these locations no woody AGB was present).

	AGB t/ha	
	Berau (n = 79)	**Kapuas Hulu (n = 41)**
Average	272.82	287.28
Minimum	5.74	1.31
Maximum	744.06	900.10
Standard Deviation	127.87	204.99
Median	274.95	236.38
Confidence Interval (95%)	28.64 (244.18-301.46)	64.70 (222.58-351.99)

As described in Chapter 2.5 the different LiDAR height metrics (QMCH and CH) were correlated at these sample plot locations in Berau and Kapuas Hulu to the AGB estimates through incorporating LiDAR point densities as weighting factor. For both districts, the AGB prediction model based on the QMCH derived better results. In Berau 58 of the 79 sample plots were used for calibration and a r2 of 0.69 was achieved. In Kapuas Hulu 32 of the 44 sample plots were used and a r2 of 0.70 was achieved. Figure 10 displays the AGB prediction models for both districts.

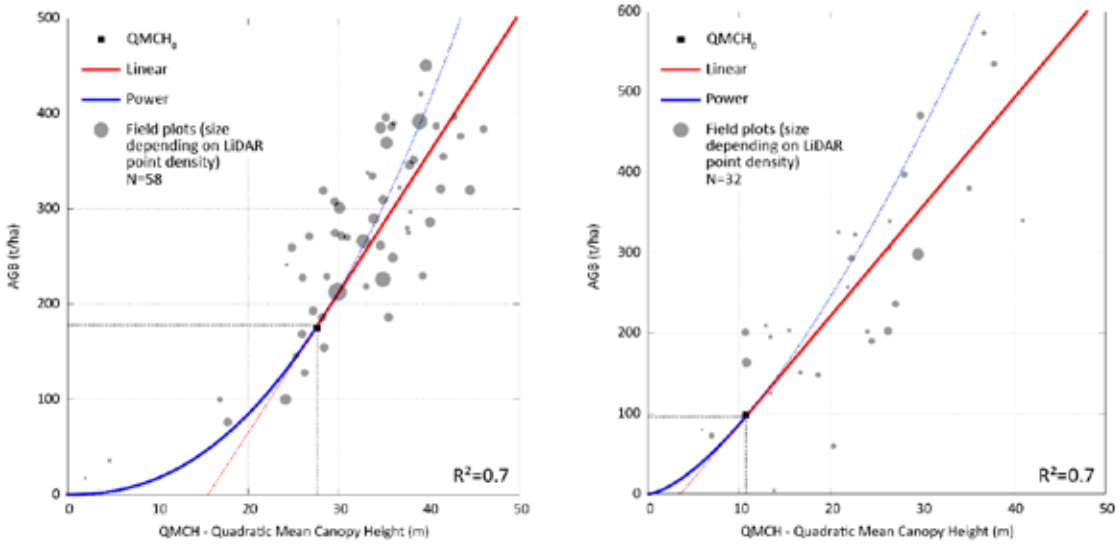

Figure 10: Predictive AGB models for the Berau (left) and Kapuas Hulu (right) forest inventory data and LiDAR dataset. The Quadratic Mean Canopy Height (QMCH) was chosen to model AGB for both district

3.3 AGB models

For each district a spatially explicit above ground biomass model was created by applying the models described in chapter 2.5. The AGB models were produced at 5 m spatial resolution i.e. each pixel represents an area of 25 m². For ease of interpretation the cell values were scaled to represent above ground biomass in t ha-1.

3.3.1 Berau

The Berau AGB model is shown in Figure 11. The vegetation cover in the Berau AGB model covers a very large AGB range, from 0 t/ha in recently cleared areas to high biomass primary forest areas with more than 550 t/ha.

The spatial distribution of AGB is highly correlated with accessibility of the area, the presence (or absence) of timber concessions and finally the topography. The AGB model covers dipterocarp dryland forest with different logging intensities, degradation stages, and an elevation range from the lowland to lower montane zones. Furthermore, the LiDAR model also covers some timber plantation areas in the south west. Figure 12- Figure 14 show some detailed examples of the AGB model in Berau.

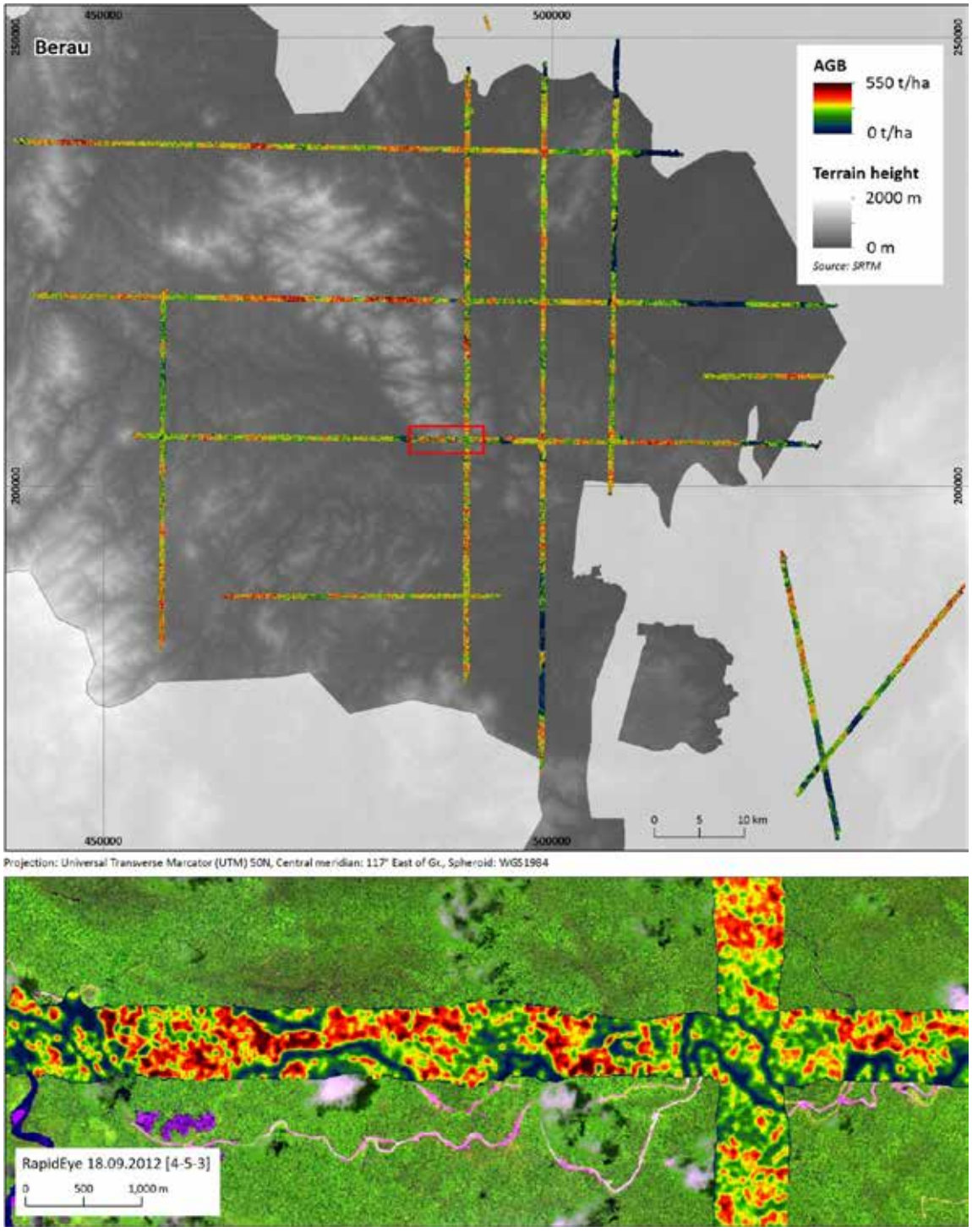

Figure 11: Example from the above ground biomass (AGB) model for Berau.

(A) RapidEye 4-5-3

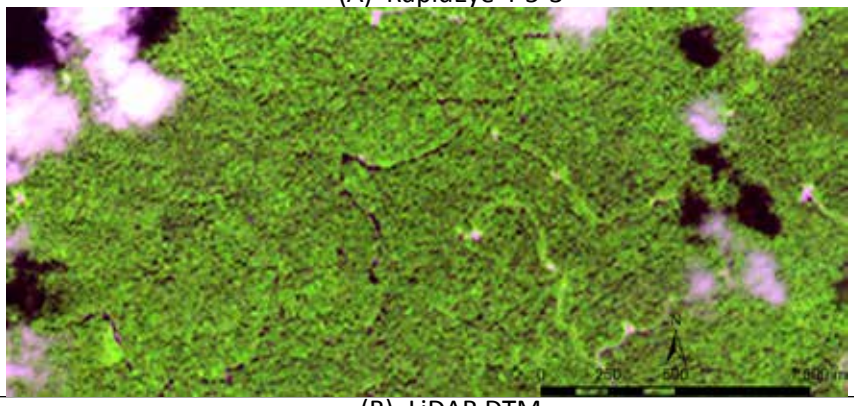

(B) LiDAR DTM

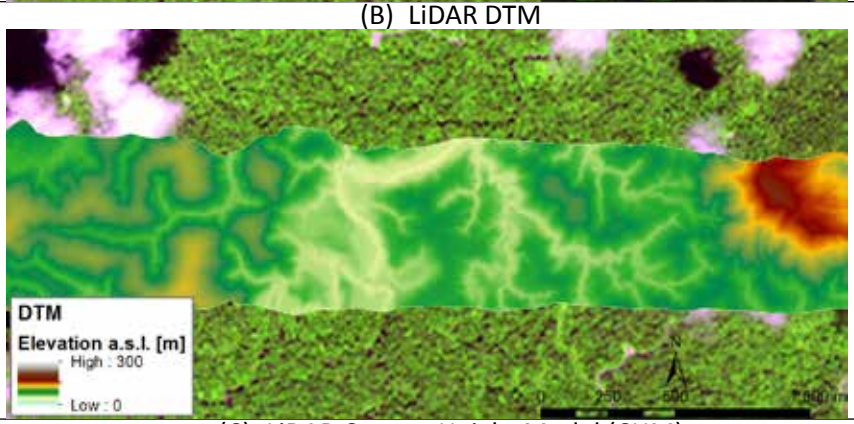

(C) LiDAR Canopy Height Model (CHM)

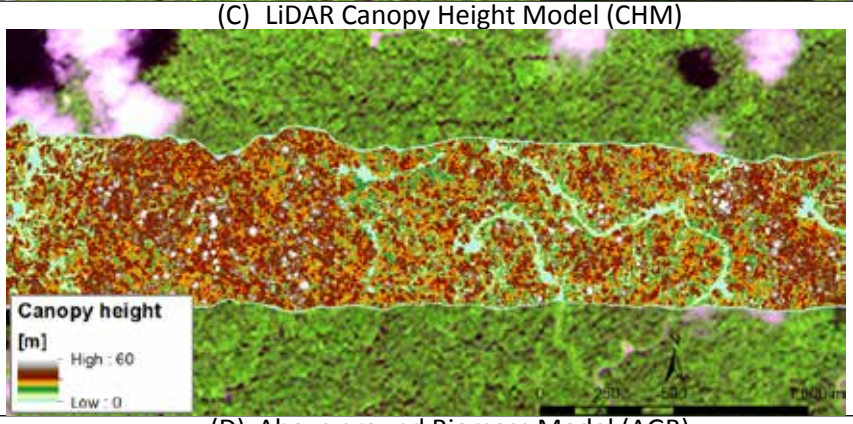

(D) Above ground Biomass Model (AGB)

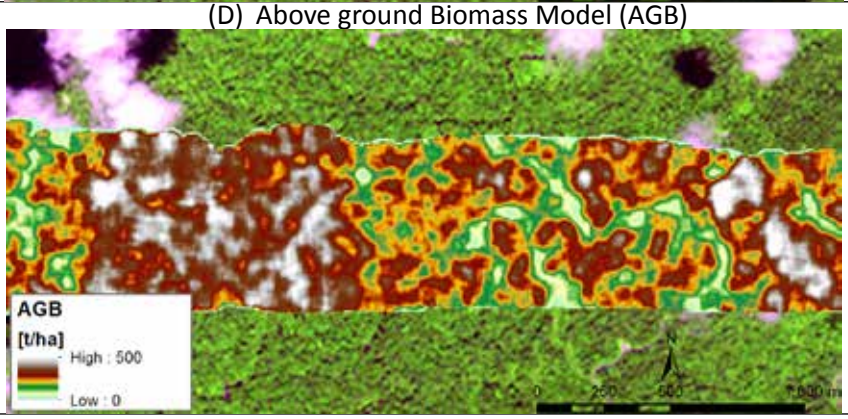

Figure 12: Example from a former logging area in Berau.

Figure 12 shows a former logging area in Berau. The logging activities were conducted in the time period 2009-2010. As plate A shows, the logging roads constructed in this area have already been largely overgrown by regenerating vegetation and the canopy damage is hardly visible in the RapidEye image. The LiDAR DTM in plate B shows topography of this example site. The area is characterized by a river in the very center, which is incised into an undulating terrain. Elevation ranges from 20 to approx. 250 m. Plate C shows the forest canopy height model.

While the forest west of the river has not been logged, and still features very high emergent trees with a height of up to 60 m, the east side of the river experienced intensive logging. This can be seen in the CHM, as all large trees have been removed and the canopy consists of low trees of up to 30 m and a lot of regenerating trees with an height of approx. 15m. However, the canopy is already closed, as the logging operations took place up until two years before data acquisition.

The AGB model in plate D very nicely reflects the impact of the logging operations on above ground biomass. While the unlogged area west of the river has an average biomass of approximately 375 t/ha, the logged over are has an average AGB of 222 t/ha. Assuming a mean annual increment of AGB after logging of 5-15 t/ha/yr, it can be derived that AGB was reduced by the logging operations to approx. 190 – 205 t/ha, i.e. approximately 170 – 185 t/ha of AGB have been extracted.

Figure 13 shows an area which was recently logged at the time of the image and LiDAR data acquisition (2012). This recent logging activity is clearly visible in the RapidEye satellite image (plate A), where the pink to purple linear structures represent large haul roads, surrounded by purple scattering in the forest canopy which shows canopy gaps as well as skid trails. The DTM (plate B) shows an undulating terrain, and that the haul roads are always constructed on the ridges while the logging is conducted in the depressions.

The canopy model (plate C) shows that the majority of large size trees have been removed during the logging activities, leaving large gaps with low or now vegetation behind. Vegetation along the haul roads is completely cleared. Directly adjacent to the south (right) is an area which has not been logged as of yet, where the tree canopy is still closed and the trees are considerably higher.

The AGB model (plate D) very clearly shows the reduced above ground biomass in the active logging area, which is on average at 180 t/ha, while the adjacent, unlogged area has a biomass of 380 t/ha on average. This confirms the extraction of approximately 200 t/ha by the logging activity, and is in line with the findings described in Figure 12.

Figure 14 shows an example of a primary forest characterized by very high trees and a consequently high above ground biomass. The area is situated in at the east side of a high mountain range. The terrain is undulating and the high biomass forest is found on both sides of an incised river bed. The forest has not been logged in the past which is reflected by abundant very large trees of up to 60 m height. These are found preferable on the slopes

of the river's v-shaped valley, while in the the lower and upper parts of the hills, the trees are smaller. Nevertheless, above ground biomass is continuously high over the whole area, amount to approximately 440 to 480 t/ha. The absence of historic and present logging activities can be explained by the remoteness and inaccessibility of this area, and therefore the forests are considered to be in primary state.

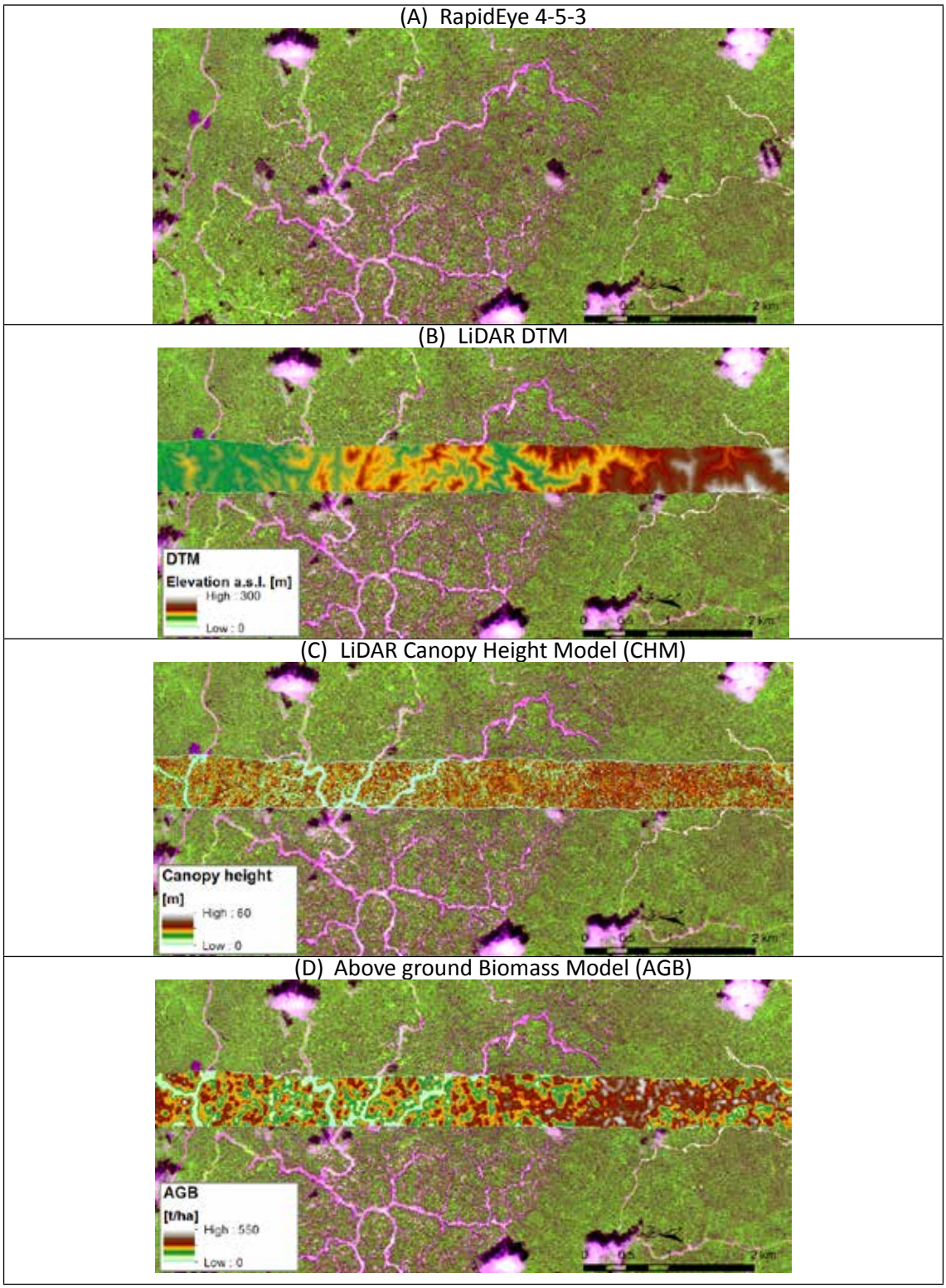

Figure 13: Example of a recently logged dryland forest area in Berau.

(A) RapidEye 4-5-3

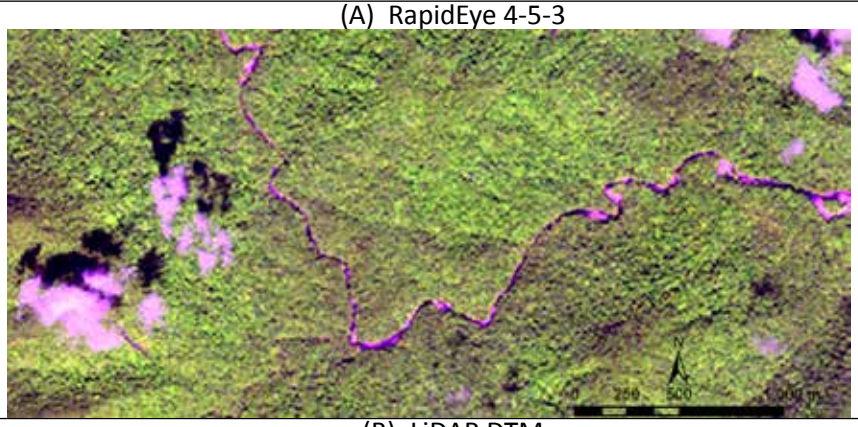

(B) LiDAR DTM

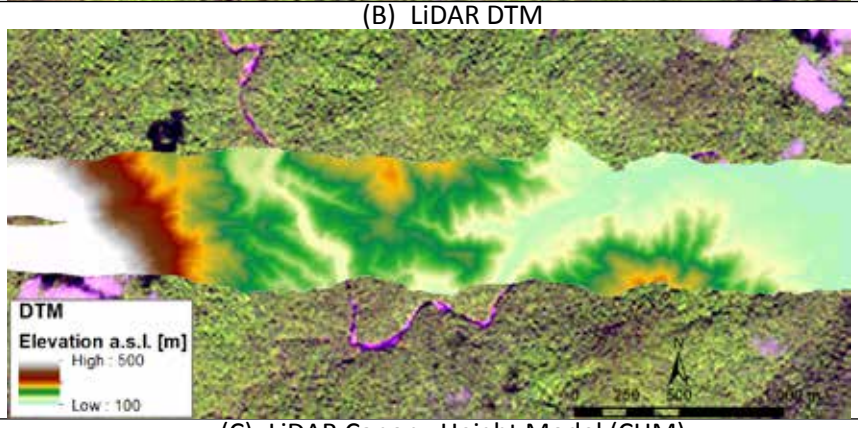

(C) LiDAR Canopy Height Model (CHM)

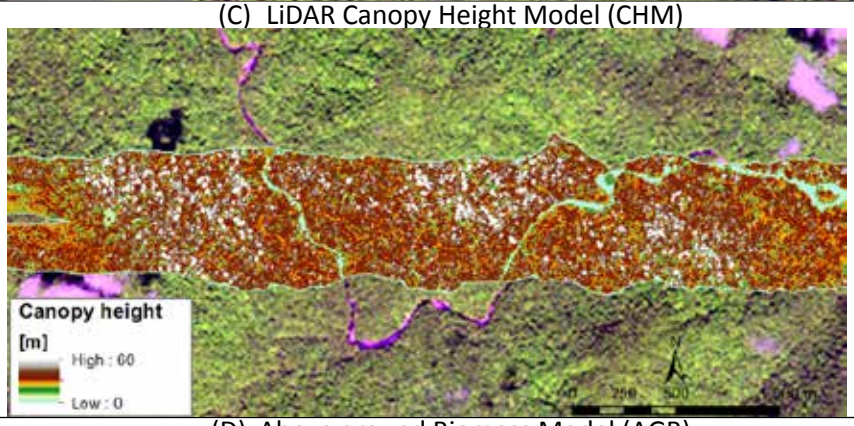

(D) Above ground Biomass Model (AGB)

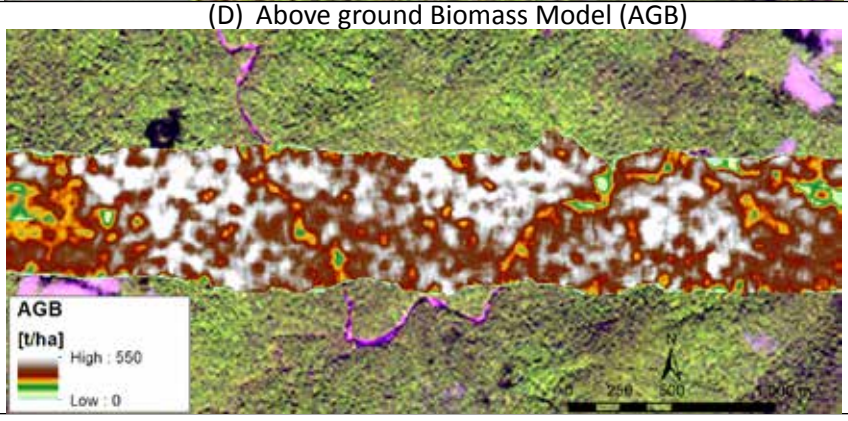

Figure 14: Example of a high biomass primary forest in Berau.

3.3.2 Kapuas Hulu

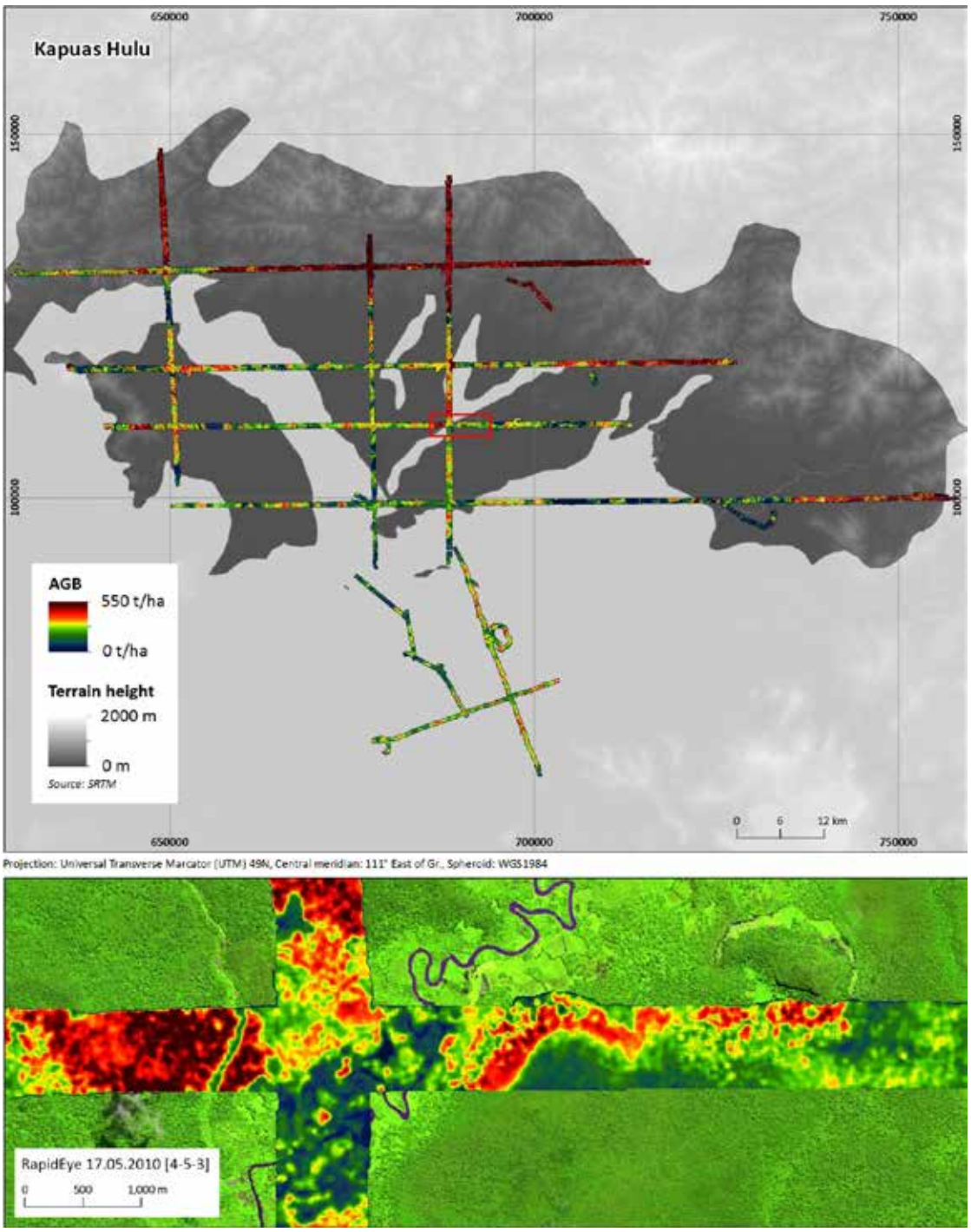

Figure 15: Example from the above ground biomass (AGB) model for Kapuas Hulu.

Figure 12 shows the final AGB model for Kapuas Hulu. The AGB distribution in Kapuas Hulu differs significantly in a couple of respects when being compared to the other two districts. This is due to the presence of a large variety of forest types on the one hand and due to the forest and land-use on the other hand.

From a land-cover perspective, the Forest Management Unit in Kapuas Hulu can be separated into two zones or strata. The uplands in the north and north-east are characterized by undulating terrain consisting of moderate to steep slopes and are covered by dipterocarp dryland forests. These forests, while been used for timber extraction with limited intensity, are characterized by a large abundance of very tall trees (>55 m), limited access and therefore considerably high biomass (partly beyond 650 t/ha).

The lowland areas in Kapuas Hulu are characterized by a patchwork of peat swamps, riparian zones and dryland areas with partly intensive land use, persistent for centuries. The peat swamp forests are characterized on the one hand by the two distinctive forest types tall to medium peat swamp forest, and low pole peat swamp forest. These types differ significantly in morphology: while the tall to medium peat swamp forest is characterized by trees of diverse heights and diameters, the low pole peat swamp forest is characterized by a very homogenous tree composition of very low trees (10-15 m in height) with small diameter. While the tall to medium peat swamp forest is commonly used for timber extraction, a primary and secondary (mostly intact and degraded) can be distinguished. Due to the very low commercial value of the trees in low pole peat swamp forests, these are commonly not logged at all, and only a primary state can be found.

The riparian zone, as well as the dryland zone, is characterized of a dense mosaic landscape of forest patches and agricultural fields, the latter consisting of rice paddies, mixed gardens and smallholder rubber plantations.

Figure 16 to Figure 19 show a set of examples from the landscape and the above ground biomass in Kapuas Hulu. The landscape in Figure 16 consists of a forest mosaic landscape located north to the village of Sadap in the Embaloh Hulu subdistrict. It is characterized by a long history of antropogenic use and consists of a patchwork of shifting cultivation, regenerating forest, agroforestry and remnant natural dryland forest patches (plate A). The natural forest is characterized by a dominance of extremely tall trees which are typical for this landscape in the mountain ranges of Kapuas Hulu. The LiDAR derived DTM in plate B shows the gently undulating terrain. The canopy height model in plate C shows the low vegetation canopy in the deforested and regrowing areas, and the very tall trees in the remnant forest patches. Tree heights in the natural forest is strongly correlated with the topography, with tall trees being found in the valley floors and smaller trees on the ridges. The forest patches are also nicely reflected in the AGB distribution shown in the AGB model in plate D, and have a very high biomass between 450 t/ha and 580 t/ha. The agroforestry patches in between have a considerably lower biomass between 150 and 250 t/ha.

Figure 17 shows a forested area which has been logged over, albeit only within a limited distance along a network of haul roads stretching into the site. Similar to the logging sites in Berau, the haul roads are usually constructed along the ridges of the undulating topography (plate A and B) with the logging being conducted on the adjacent downward slopes. This is reflected by the replacement of tall trees by canopy gaps on both sides of the road (plate C) and also clearly visible in the AGB model (plate D). AGB in these logging area is still very high, even after loggin, at between 300 and 400 t/ha. However, the unlogged areas adjacent to the logging blocks have an even higher biomass at between 600 and 650 t/ha, due to abundant very tall trees of over 60-65 m height.

(A) RapidEye 4-5-3

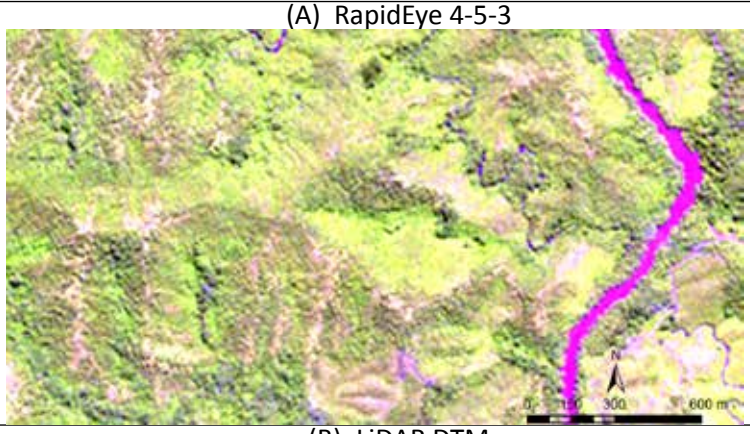

(B) LiDAR DTM

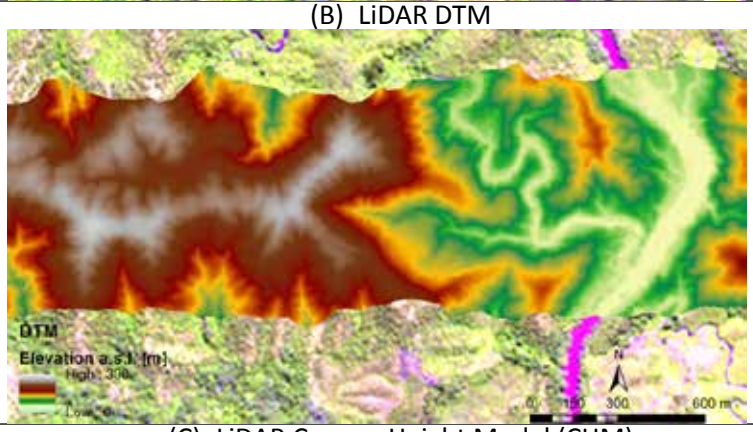

(C) LiDAR Canopy Height Model (CHM)

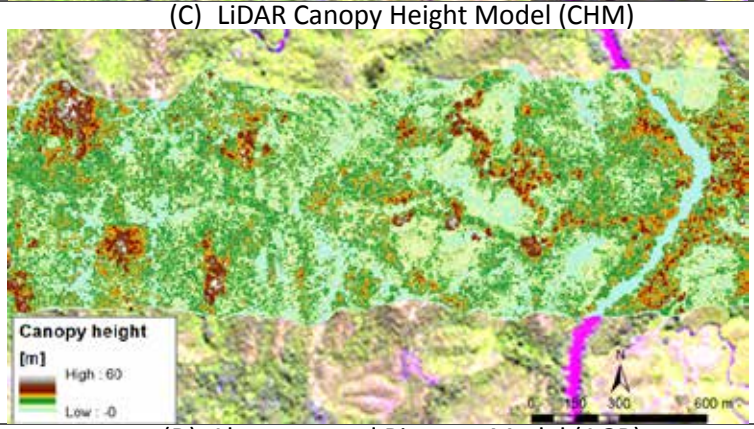

(D) Above ground Biomass Model (AGB)

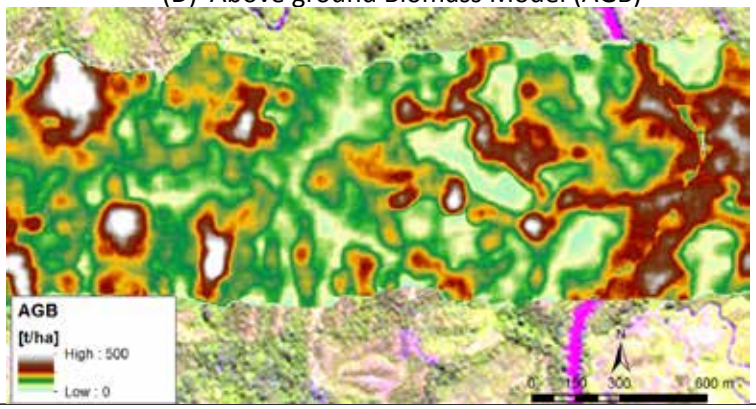

Figure 16: Example of a fragmented dryland forest mosaic from Kapuas Hulu.

(A) RapidEye 4-5-3

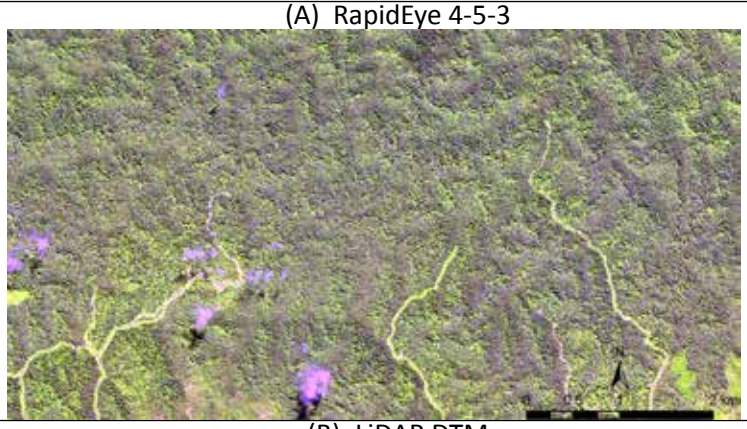

(B) LiDAR DTM

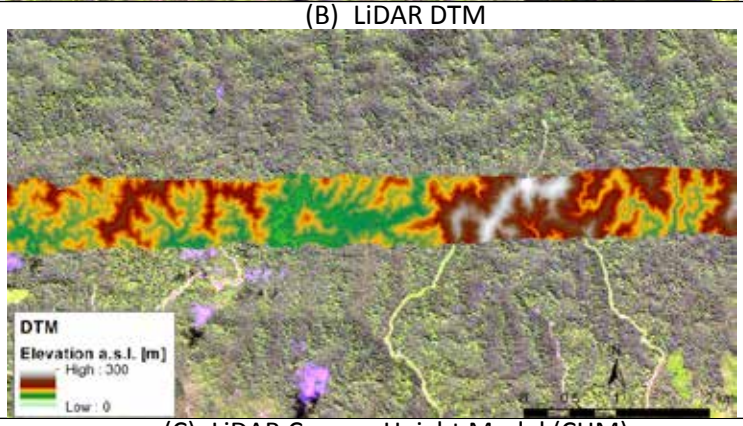

(C) LiDAR Canopy Height Model (CHM)

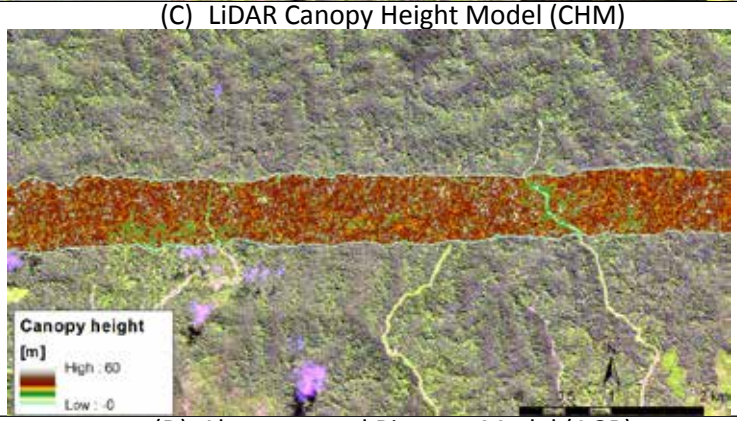

(D) Above ground Biomass Model (AGB)

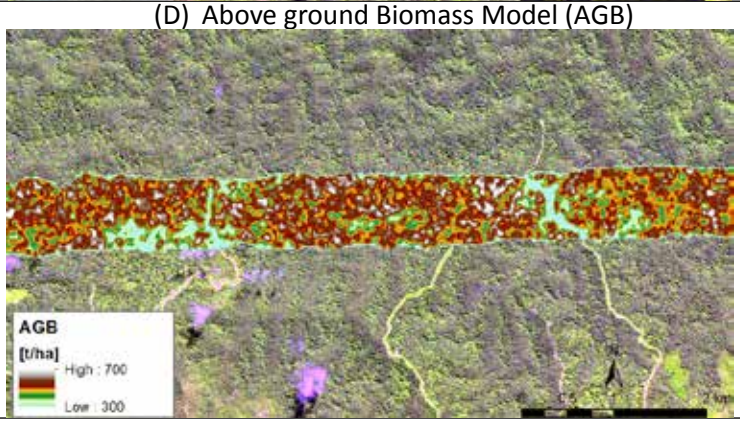

Figure 17: Example from a logged over dryland forest in Kapuas Hulu.

(A) RapidEye 4-5-3

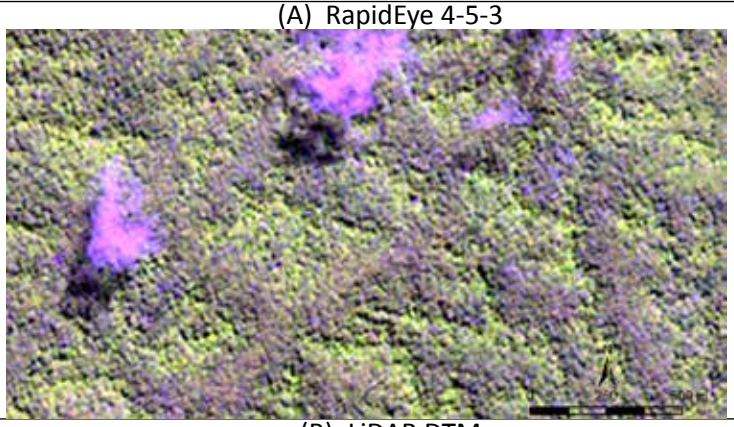

(B) LiDAR DTM

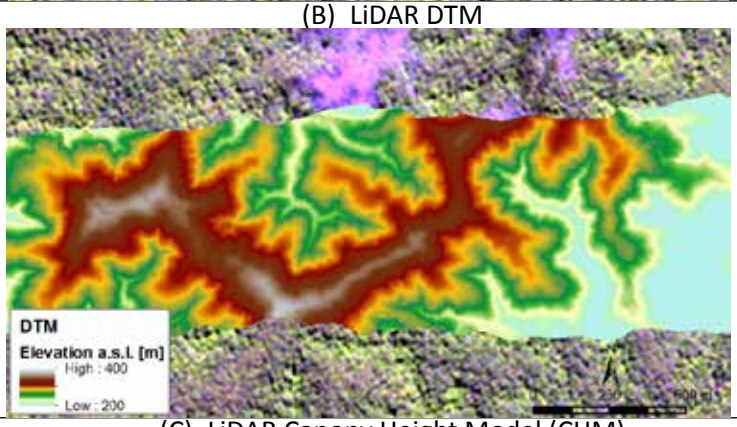

(C) LiDAR Canopy Height Model (CHM)

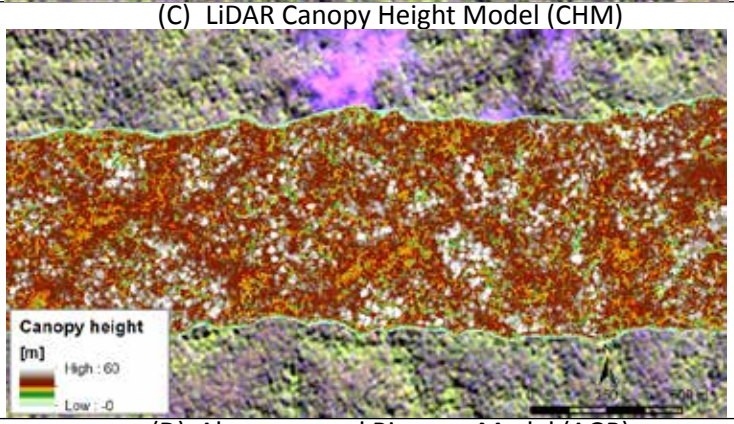

(D) Above ground Biomass Model (AGB)

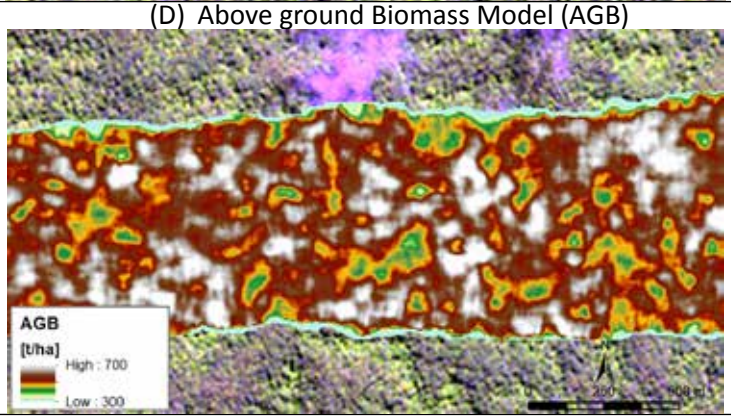

Figure 18: Example from a high biomass dryland forest in Kapuas Hulu.

Figure 18 shows a high biomass dryland forest in the uplands of Kapuas Hulu, which has not been logged. The CHM (plate C) shows that there are abundant tall trees of 60m height and more. When being compared to the DTM (plate B), it becomes clear that the tall trees are found preferably in the depressions of the undulating terrain, while the smaller trees are concentrated on the ridges. AGB ranges in this area between 580 t/ha and 635 t/ha.

Finally, Figure 19 shows a an example from a peat swamp area in Kapuas Hulu west of the Embaloh river. This peat swamp forest consists of a variety of very distinct forest sub-types and degradation stages. The satellite image in plate A shows in tall- to medium peat swamp forest along the northern bounds of the forest, with different impacts of selective logging (expressed by the different shades of green).

In the lower center of the images, there is a low pole peat swamp forest represented by the flatly textured purple color in the satellite image. A look at the DTM shown in plate B shows the very gently sloping but generally flat topography of the ombrogenic peat dome.

The DTM also shows that the low pole forest is situated in a depression, which causes the site to be extensively waterlogged most of the time, which is the reason for the development of this specific forest type. The CHM (plate C) shows that tree height is typically very much lower in the low pole peat swamp forest (at 10-15 m height) than in the tall to medium peat swamp forest (which is between 20 and 35 m, with a few emergents even exceeding that).

These differences are also very well expressed in the AGB model (plate D). While the low pole peat swamp forest in this area is characterized by average AGB values ranging from approx. 200 t/ta to 220 t/h, the tall to medium peat swamp forest features AGB values between 410 and 440 t/ha.

(A) RapidEye 4-5-3

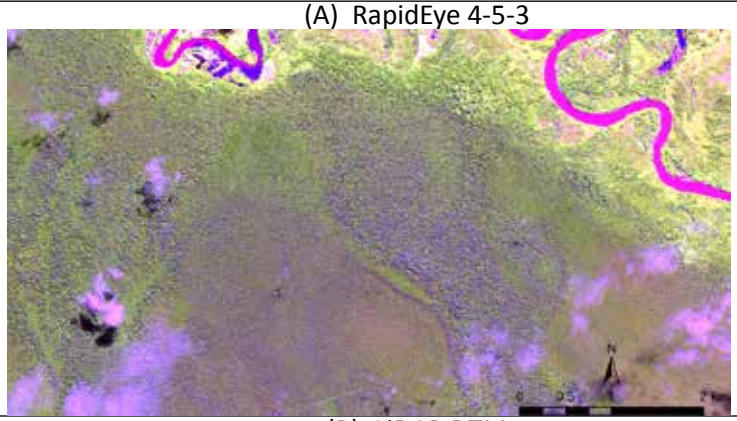

(B) LiDAR DTM

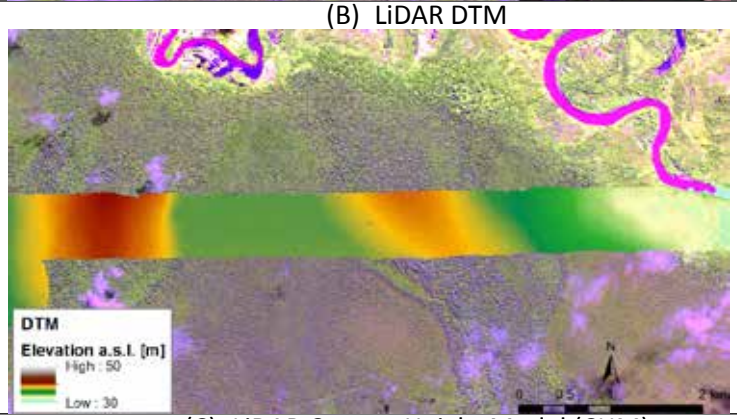

(C) LiDAR Canopy Height Model (CHM)

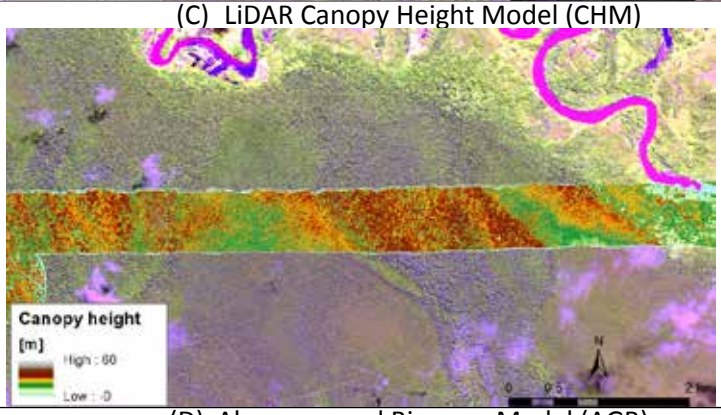

(D) Above ground Biomass Model (AGB)

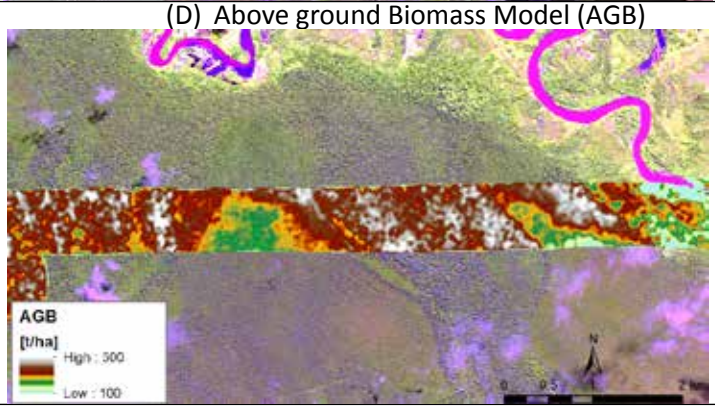

Figure 19: Example from a peat swamp forest in Kapuas Hulu, showing different types of peat swamp forest.

3.4 Land cover map Berau Forest Management Unit

Table 7: Spatial extent of the different land cover classes in the Berau Forest Management Unit.

Land cover class	Area (ha)	%
Primary lowland forest	48,127	6.1%
Secondary lowland forest	277,266	35.3%
Primary hill and submontane forest	210,003	26.7%
Secondary hill and submontane forest	78,573	10.0%
Primary lower montane forest	59,847	7.6%
Secondary lower montane forest	3,515	0.4%
Upper montane forest	4,281	0.5%
Shrubs, shifting cultivation, smallholder agriculture, grassland	19,512	2.5%
Oil palm plantation	21	0.0%
Timber plantation	6,484	0.8%
Settlement	39	0.0%
Bare area	6,886	0.9%
Water	2,261	0.3%
No data	69,206	8.8%
Total	**786,021**	**100.0%**

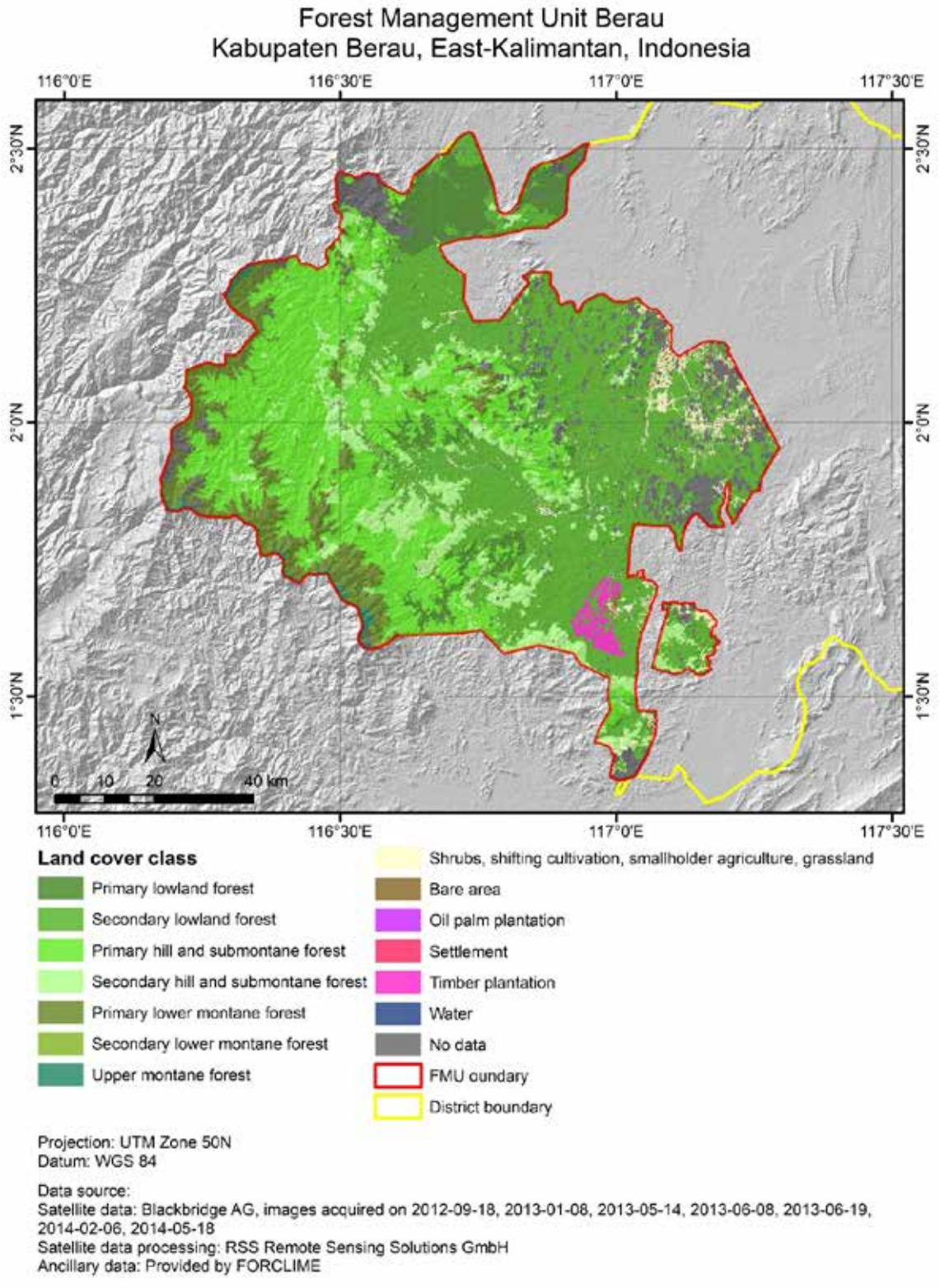

Figure 20: Land cover map of the Berau Forest Management Unit.

3.5 AGB values for the different land cover categories

In order to derive local AGB values for the different land cover categories in each district, the spatial AGB models were overlaid with a high resolution land cover map of each district. For Berau, the land cover map presented in chapter 3.3 was used.

For Malinau and Kapuas Hulu, comparable land cover maps, also based on RapidEye satellite imagery were already available from a previous assessment by RSS in the FORCLIME programme. The maps are documented in the FORCLIME "Final Report for the RapidEye high resolution land cover classification and forest benchmark map for the Forest Management Units in Kapuas Hulu and Malinau". The land cover maps are shown in Figure 21 and Figure 22.

Table 8 and Table 9 show the local AGB values derived for the two districts Berau and Kapuas Hulu. As the forest inventory in Malinau was not completed to date, no AGB data is avaible yet. Note that AGB values were only derived for those land cover types that were covered with both, LiDAR data and land cover data. Further, timber and oil palm plantations were excluded from the analysis as those plantations have rotation cycles and a LiDAR derived AGB value would always only cover one specific point in time in this rotation cycles. For these land uses, an average AGB value, considering the whole rotation cycle seems more appropriate.

Table 8 shows the AGB values for Berau. The highest biomass is found in Primary Hill and Submontane Forest with 337 t/ ha on average, followed by Primary Lowland Forest with 319 t/ha. These values are, for primary dryland forest types in Kalimantan, considered as rather low. Reasons for low biomass might ly in a confusion of primary and secondary forest in the land cover classification, as a forest degradation which has happened a long time in the past might not always be detectable in the recent satellite image.

Compared to the primary forest types, the secondary forest classes of hill and submontane forest and lowland forest have AGB values of 295 t/ha and 291 t/ha. These values are as expected for logged over forests, especially as the secondary forest classes contain all kinds of recovery stages. While recently logged forest will have an AGB much lower then that, a secondary forest which has already had sufficient time to recover will have an AGB in the range of the detected values. As large parts of the area of LiDAR coverage are being logged already since many years, these average values are considered fully acceptable.

The AGB values calculated for Kapuas Hulu differ significantly from those in Berau (Table 9), similarly to what has been observed already in the forest inventory data (chapter 3.2). The highest biomass values are found in the Primary Hill and Submontane and Primary Lowland Forest classes with 515 t/ha and 512 t/ha on average. This might seem very high at first sight, however, the abundance of very tall trees with more than 60m height is remarkable in Kapuas Hulu. This is also reflected in the results of the field inventory (chapter 3.2).

While the AGB values for primary forests are very similar between the hill and submontane zone and the lowland zone, the AGB for secondary forests differ significantly with 397 t/ha and 330 t/ha. This can be explained by differences in the logging impact in these zones. While the lowland forest is genererally more accessible and therefore allows for a more effective timber extraction, logging in the hill and submontane zone is more complicated, and therefore less timber is extracted.

The peat swamp forest differs significantly in AGB content in comparison to the dryland forest types. Primary peat swamp forest (of the tall to medium tall PSF subtype) has an average AGB od 323 t/ha, while secondary swamp forest has an average AGB of 296 t/ha. The value for secondary peat swamp forest is considered very high, which can be explained by the long time period since the degradation by logging took place in the investigated area. This results in a long period of recovery, and therefore the AGB high. Primary low pole peat swamp forest, a subtype which is characterized by very small, pole-like trees, has an average AGB of 178 t/ha. This shows that, for an accurate assessment of AGB of peat swamp forest, it is of urgent importance to discriminate these forest subtypes in order not to introduce large uncertainties. The large differene in AGB, in combination with the absence of a secondary/degraded low pole peat swamp forest class, necessitates this discrimination. If the two primary peat swamp forest types would be combined, and the AGBs averaged, the result would be a lower AGB for primary than for secondary peat swamp forest.

The class Shrubland, shifting cultivation, smallholder agriculture, grassland has a considerably higher biomass in Kapuas Hulu than in Berau, due to a dominance of smallholder rubber plantations in this class.

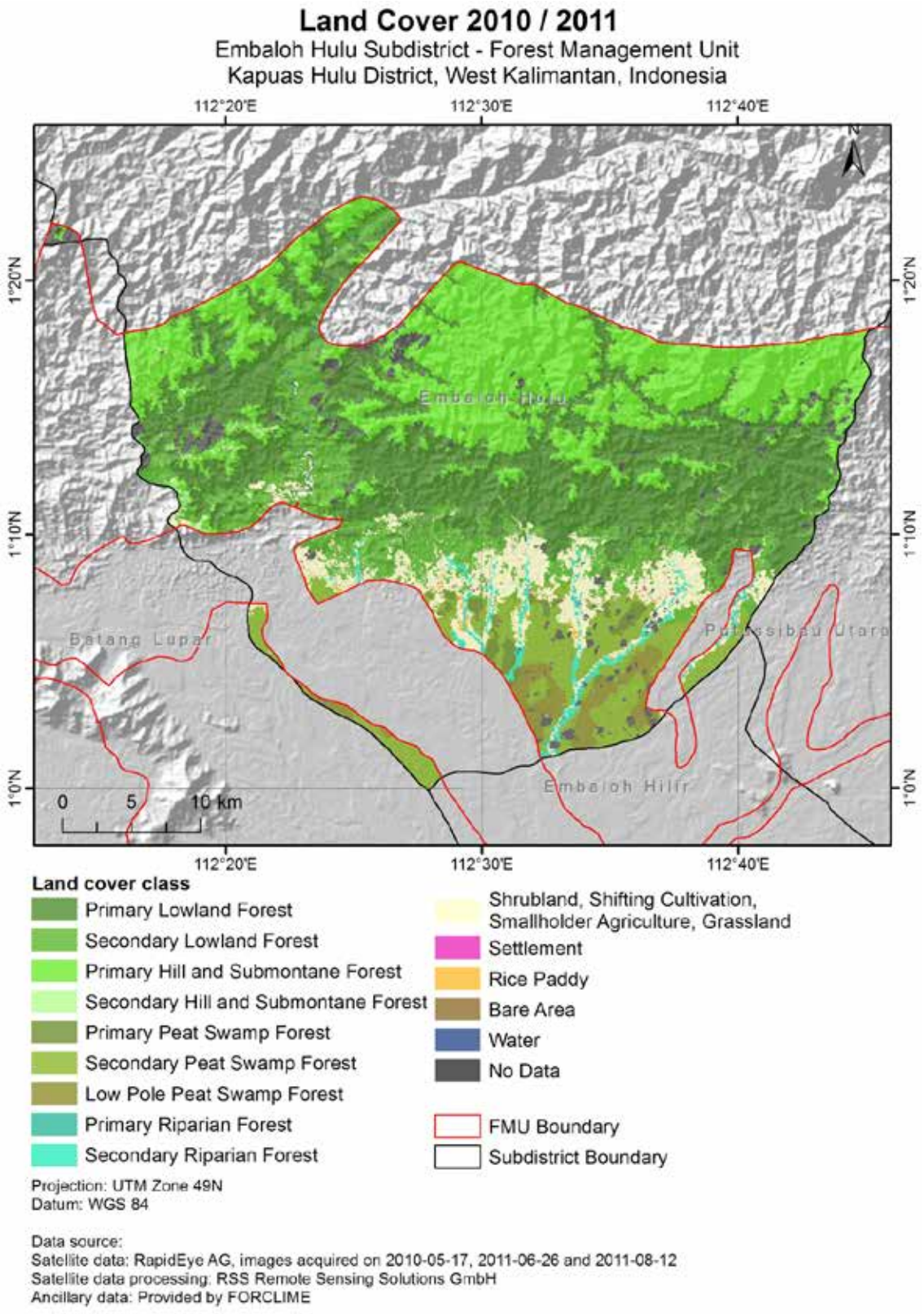

Figure 21: Land cover map of the Embaloh subdistrict in the Forest Management Unit of Kapuas Hulu.

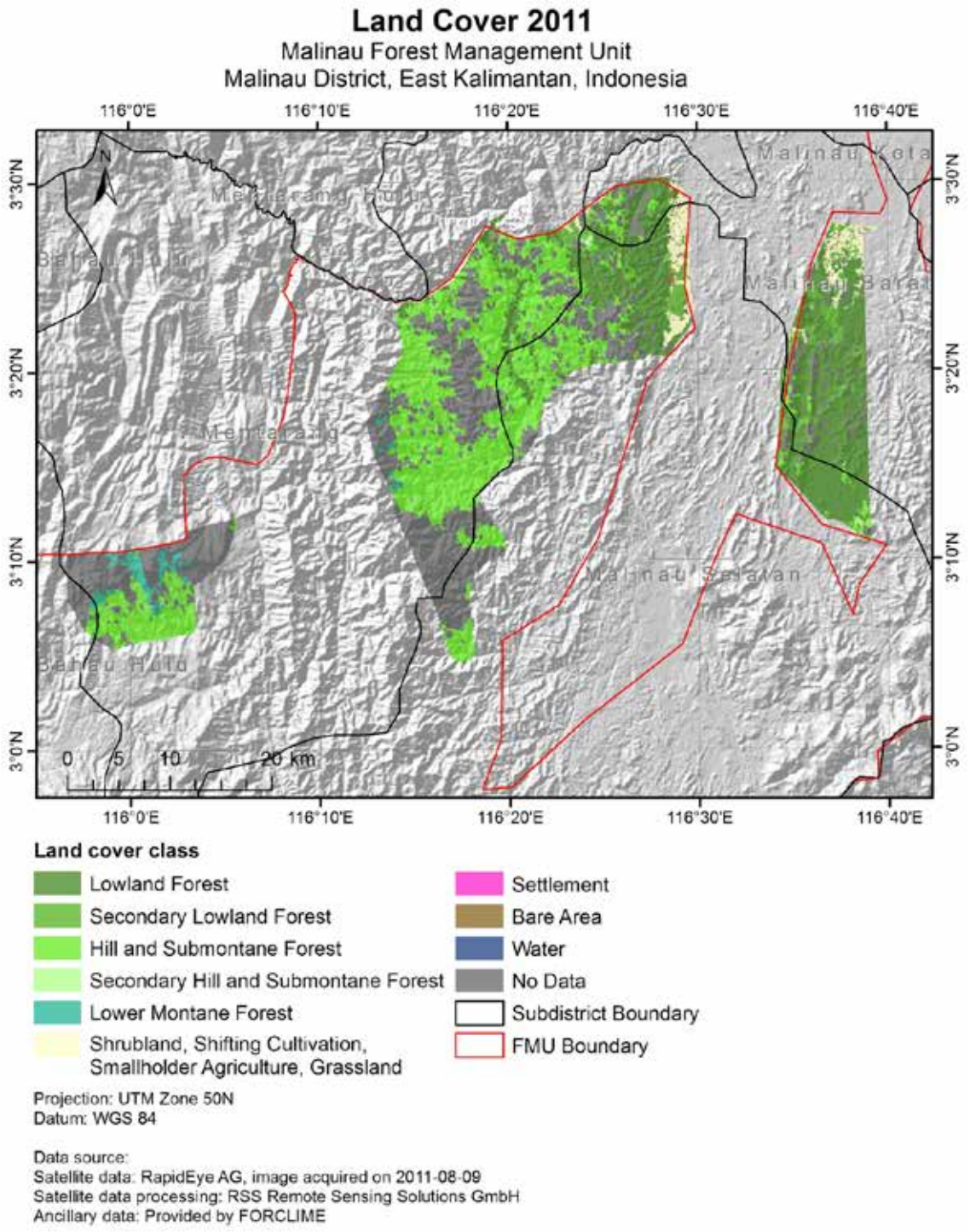

Figure 22: Land cover map of the Forest Management Unit in Malinau.

Table 8: Local AGB values derived from the LiDAR AGB model for Berau.

BERAU	**Above ground Biomass [t AGH ha-1]**				
FORCLIME classification scheme	Average	SD	Min	Max	Sample Count
Primary Lowland Forest	**319**	103.86	23.45	711.77	13,832
Secondary Lowland Forest	**291**	89.84	0.06	677.93	292,811
Primary Hill and Submontane Forest	**337**	92.99	21.69	729.84	48,689
Secondary Hill and Submontane Forest	**295**	105.01	1.75	718.97	48,015
Primary Lower Montane Forest	**226**	47.16	96.49	291.47	51
Secondary Lower Montane Forest	**103**	21.61	61.58	124.77	11
Settlement	**4**	0.00	3.53	3.53	1
Shrubs, Agriculture, Grassland, Wetland, Non-Forest vegetation	**61**	89.80	0.01	496.62	8,412

Table 9: Local AGB values derived from the LiDAR AGB model for Kapuas Hulu.

KAPUAS HULU	**Above ground Biomass [t AGH ha-1]**				
FORCLIME classification scheme	Average	SD	Min	Max	Sample Count
Primary Lowland Forest	**512**	85.19	122.41	1073.17	79,101
Secondary Lowland Forest	**330**	123.55	1.37	758.77	11,352
Primary Hill and Submontane Forest	**515**	89.03	168.01	865.08	13,880
Secondary Hill and Submontane Forest	**397**	119.50	158.45	798.27	335
Primary Peat Swamp Forest	**323**	67.46	74.37	485.39	1,076
Secondary Peat Swamp Forest	**296**	74.67	0.25	555.41	12,828
Primary Low Pole Peat Swamp Forest	**178**	86.31	41.86	469.64	6,871
Secondary Riparian Forest	**249**	87.66	2.76	465.07	339
Shrubs, Agriculture, Grassland, Wetland, Non-Forest vegetation	**107**	71.66	0.00	374.86	1,952

It has to be noted again that not all land cover types present in three districts have been covered by the analysis presented here. This means that, for a complete AGB assessment on district scale, the local AGB values need to be complemented by values derived from other sources, such as the scientific literature. AGB values of all land cover types mapped in the tree districts can be found in the report "Survey on the Land Cover Situation and Land-Use Change in the Districts Kapuas Hulu and Malinau, Indonesia - Final Report for assessment of district and KPH wide REL assessment", prepared by RSS in the framework of a previous study (Rss GmbH 2012-2).

4 Summary and conclusions

This study demonstrates the establishment of above ground biomass and carbon model for three districts in Kalimantan based on LiDAR technology together with forest inventory data. The methodology applied in this study was used to derive accurate local AGB values for a MRV system to quantify biomass and carbon stock changes in the three districts of Kapuas Hulu, Berau and Malinau. The methodology can be upscaled and adapted to province or national scale.

For each of the Forest Management Units (FMUs), approximately 500 km of LiDAR transects have been acquired in the framework of this study. The data was processed in a first step into common data products, such as a Digital Surface Model (DSM), a Digital Terrain Model (DTM) and Canopy Height Models (CHM). In combination with high quality forest inventory data collected by FORCLIME in Berau and Kapuas Hulu, LiDAR based AGB prediction models were developed for the two districts. These models, applied to the normalized LiDAR point cloud data were then used to create spatially explicit AGB models with a dense sampling density of 5m for the whole LiDAR datasets.

Superimposed with a high resolution land cover classifiacation based on 5m RapidEye satellite imagery, local AGB values were derived from the AGB models for each district.
The magnitude of AGB of the different forest types varied considerably between the districts. This was already indicated in the field data, which showed that the same forest types have a considerably higher biomass in Kapuas Hulu than in Berau, due the much higher abundance of tall trees. Another factor influencing the average AGB density in the districts is the history and intensity of timber extraction in the two districts. As commercial logging has already a long history in Berau, the majority of secondary forests in Berau have been able to recover and have thus only 10% less AGB than their primary form. In Kapuas Hulu, it was found that the secondary forest had an AGB of about 30-40 % less than the primary form.

The differences found in the different districts underline the necessity of locally adjusted AGB assessments in order to produce accurate and reliable emission estimates with low uncertainties.

5 References

Asner, G.P., G.V.N. Powell, J. Mascaro, D.E. Knapp, J.K. Clark, J. Jacobson, T. Kennedy-Bowdoin, A. Balaji, G. Paez-Acosta, E. Victoria, et al. 2010. High-resolution forest carbon stocks and emissions in the Amazon. Proceedings of the. Nationall. Academy. of Sciences of the United States of America. 107, 16738–16742.

Asner, G.P., J. Mascaro, H.C. Muller-Landau, G. Vieilledent, R. Vaudry, M. Rasamoelina, J.S. Hall and M. van Breugel. 2012. A universal airborne LiDAR approach for tropical forest carbon mapping. Oecologia 168, 1147–1160.

Ballhorn U., Jubanski J., Siegert F., (2011). ICESat/GLAS Data as a measurement tool for peatland topography and peat swamp forest biomass in Kalimantan, Indonesia. Remote Sens. 3, 1957–1982.

Brown, S. 1997. *Estimating biomass and biomass change of tropical forests: A primer.* FAO Forestry paper, 134, 1-84.

Chave, J., C. Andalo, S. Brown, M.A. Cairns, J.Q. Chambers, D. Eamus, H. Folster, F. Fromard, N. Higuchi, T. Kira, et al. 2005. Tree allometry and improved estimation of carbon stocks and balance in tropical forests. Oecologia 145, 87–99.

Englhart S., Jubanski J., Siegert F., (2013). Quantifying Dynamics in Tropical Peat Swamp Forest Biomass with Multi-Temporal LiDAR Datasets. Remote Sens. 5, 2368–2388.

Franke J., P. Navratil, V. Keuck, K. Peterson, F. Siegert (2012). Monitoring fire and selective logging activities in tropical peat swamp forests. IEEE Journal of Selected Topics in Applied Earth Observations and Remote Sensing, Vol. PP, no.99, pp.1-10, doi: 10.1109/JSTARS.2012.2202638.

Jubanski J., Ballhorn U., Kronseder K., Siegert F., (2013). Detection of large above-ground biomass variability in lowland forest ecosystems by airborne LiDAR. Biogeosciences 10, 3917–3930.

Kraus 1998

Kronseder K., U. Ballhorn, V. Böhm, F. Siegert, 2012. Above ground biomass estimation across forest types at different degradation levels in Central Kalimantan using LiDAR data. International Journal of Applied Earth Observation and Geoinformation, 18, 37-48.

Lackman, S. 2011. Good Practice in designing a Forest Inventory. Regional Workshop: Capacity Development for sustainable National Green-House Gas Inventories – AFOLU Sector, (CD REDD II) Programme.

Pfeifer. N.. Stadler. P. & Briese. C. 2001. Derivation of digital terrain models in SCOP++ environment. OEEPE Workshop on Airborne Laserscanning and Interferometric SAR for Detailed Digital Elevation Models. Stockholm.

Richter R., Schläper D., (2014). Atmospheric / Topographic Correction for Satellite Imagery.

RSS GmbH, 2012. Final Report for the RapidEye high resolution land cover classification and forest benchmark map for the Forest Management Units in Kapuas Hulu and Malinau. Baierbrunn.

RSS GmbH, 2012. Survey on the Land Cover Situation and Land-Use Change in the Districts Kapuas Hulu and Malinau, Indonesia - Final Report for assessment of district and KPH wide REL assessment. Baierbrunn.

Zanne, A.E., Lopez-Gonzalez, G., Coomes, D.A., Ilic, J., Jansen, S., Lewis, S.L., Miller, R.B., Swenson, N.G., Wiemann, M.C., Chave, J. 2009. Global wood density database. http://hdl.handle.net/dryad.235.

Appendix

Appendix to the final report: AGB model for Malinau from final forest inventory data

1. Field inventory data used for AGB prediction models

The location of the nested field plots for Malinau (25 plots) are shown in Figure A1. As indicated by the red crosses, nine plots were not considered for the AGB prediction model. Two further plots (purple crosses) were located outside the LiDAR track.

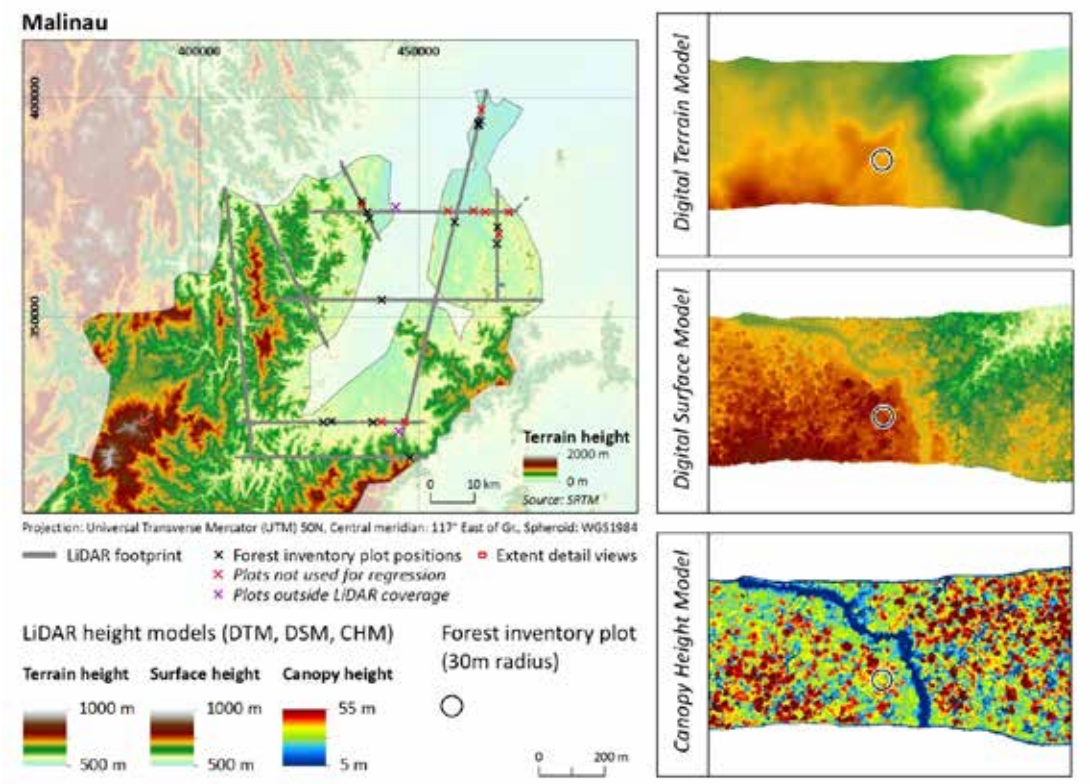

Figure A1: Example from the LiDAR products generated for Malinau. Also shown are the positions of the 25 forest inventory plots.

Table A1 additionally displays the descriptive statistics considering AGB estimates from this forest inventory.

Table A1: Descriptive statistics considering Above Ground Biomass (AGB) estimates from the forest inventory in Malinau (nine inventory plots excluded).

	AGB t/ha
	Malinau (n = 14)
Average	229.30
Minimum	53.16
Maximum	547.74
Standard Deviation	120.79
Median	190.79
Confidence Interval (95%)	69.74 (159.56-299.04)

The reasons for the exclusion of the nine plots were as follows:

- For the plots SLDF 1, SLDF 6 and LDF 8 no slope information was recorded during field inventory. It is not possible to reconstruct with certainty whether there is no slope or it was just not noted in the field inspection sheet and in this case, whether a slope correction was applied or not. Since the DTM is partially indicating a considerable slope, we excluded these plots from the regression analysis.
- In plot LDF 12 only two trees were measured, which is contradicting strongly with the number of trees visible in the Canopy Height Model (Figure A2). The reason is that this plot has been logged intensively in 2014 (between the LiDAR survey and the inventory campaign) and had to be exluded from the analysis.

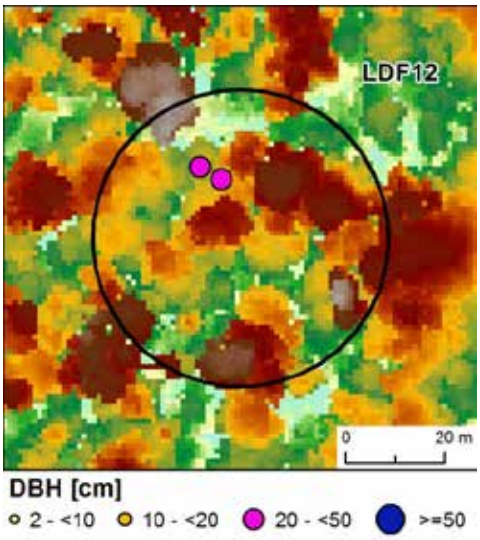

Figure A2: Plot LDF 12 with only two trees measured during forest inventory. (The black circle indicates the area of the largest nest with a radius of 30 m).

- Plot SFSF 1 is not completely covered by the LiDAR dataset and can therefore not be considered in the regression analysis (Figure A3).

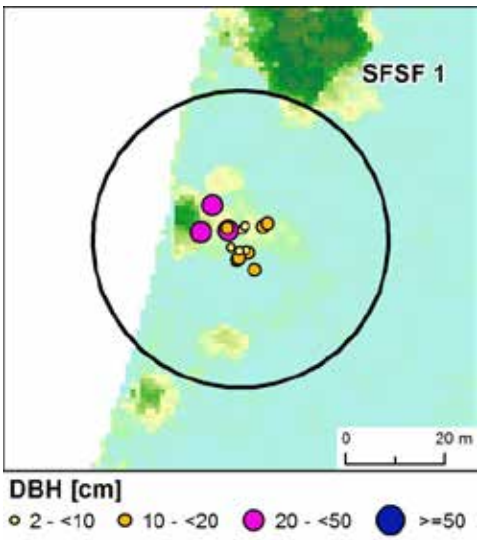

Figure A3: Location of plot SFSF 1, not completely covered by the LiDAR dataset. (The black circle indicates the area of the largest nest with a radius of 30 m).

- Plots LDF 2, 5, 9 and 10 had to be excluded due to conspicuously low AGB values measured in the field, while having high Quadratic Mean Canopy Heights.

The Quadratic Mean Canopy Height (QMCH) derived from the LiDAR point cloud was correlated at the remaining sample plot locations in Malinau to the AGB estimates through incorporating LiDAR point densities as weighting factor. 14 of the 25 sample plots were used for calibration, resulting in a R^2 of 0.49 and a RMSE of 96.95 t/ha. Figure 10A4 displays the AGB prediction model for the district Malinau.

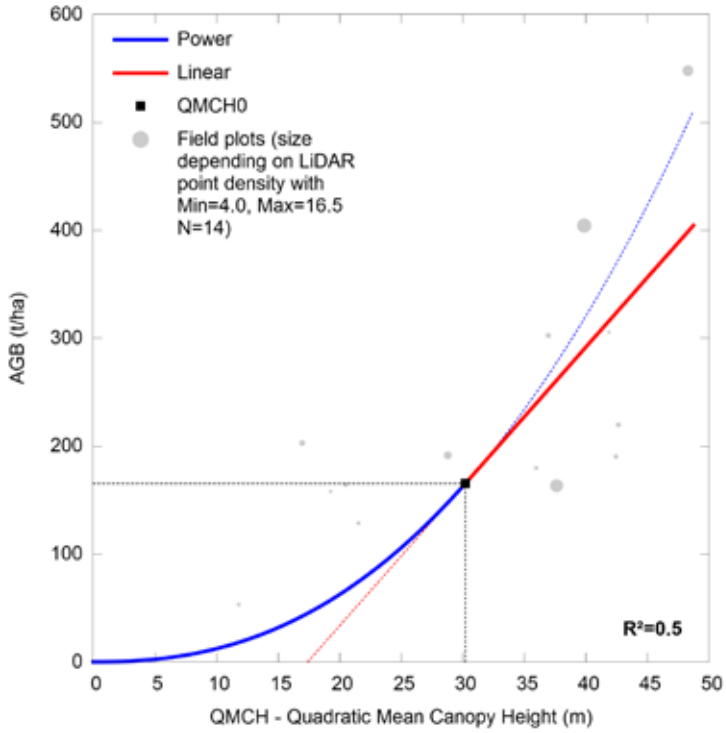

Figure A4: Predictive AGB model for the Malinau forest inventory data and LiDAR dataset.

The potential reasons for the comparably poor fit of the model were thoroughly investigated. The main problem is very likely the lacking precision of the plot center coordinates recorded by the GPS. An exact geolocation of the plots is an essential requirement for an accurate calibration of the LiDAR data.

On the one hand, a highly undulating terrain with steep slopes as found in Malinau can lead to a reduced number of satellite signals receivable by the GPS device and/or a clustered location of those signals.

On the other hand, a visual inspection of the recorded GPS tracks indicates that some problems occurred during the long-term measurement of the fixed positions and the subsequent averaging, resulting in an insufficient accuracy of the plot position. In Figure A5, this issue is demonstrated. In some plot locations, there is a shift of the location of the sample plot when compared to the long term tracklog measurements, in other instances, no long term track logs was recorded at all, which indicates that the GPS was not averaging the location of the plot center, which again can lead to severe errors in measurement.

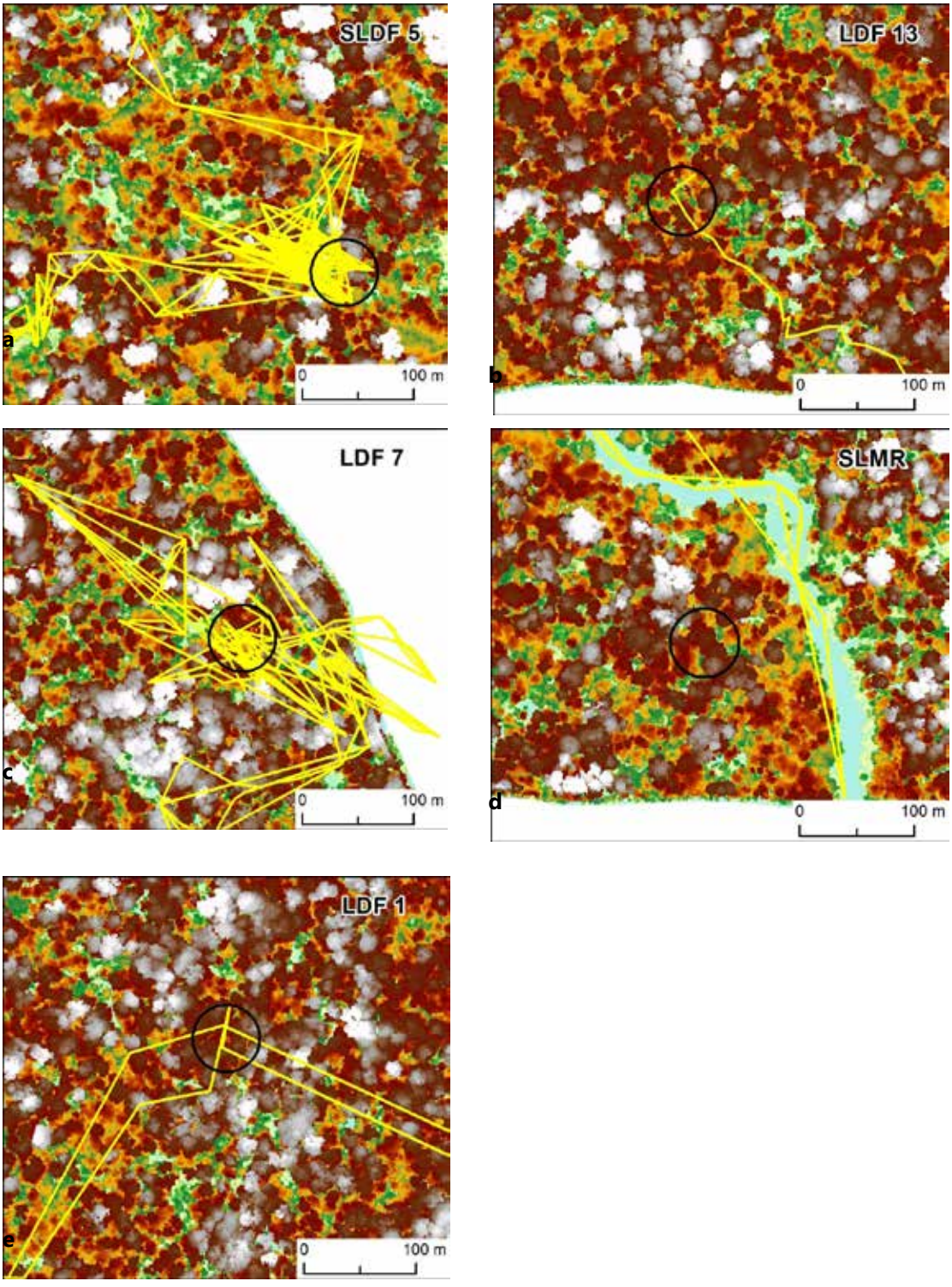

Figure A5: Examples of forest inventory plot locations (black circles) in relation to GPS tracks (yellow lines). a) Plot location is shifted from the focal point of the GPS track. b) Discontinued GPS signal. c) Individual measurements with strong discrepancies. d) No track measurements at plot location. e) No long-term measurements. f) Plot located in the center of the long-term measurements.

2. AGB models

A spatially explicit above ground biomass model was created by applying the model described in chapter 6.1. The AGB model was produced at 5 m spatial resolution i.e. each pixel represents an area of 25 m^2. For ease of interpretation the cell values were scaled to represent above ground biomass in t ha^{-1}.

3. AGB values for the different land cover categories

In order to derive local AGB values for the different forest types, the spatial AGB model was overlaid with a high resolution land cover map.

Table 8A2 the local AGB values derived from the LiDAR AGB model. Non-forest land cover types were excluded from the analysis as those typically have rotation cycles and a LiDAR derived AGB value would always only cover one specific point in time in this rotation cycles.

Table A2: Local AGB values derived from the LiDAR AGB model for Malinau.

MALINAU	**Above ground Biomass [t AGH ha-1]**				
FORCLIME classification scheme	Average	SD	Min	Max	Sample Count
Primary Lowland Forest	**281**	108.42	0.32	751.93	32,630
Secondary Lowland Forest	**201**	85.67	14.35	550.62	5,201
Primary Hill and Submontane Forest	**316**	99.98	27.04	800.94	27,212
Secondary Hill and Submontane Forest	**274**	120.49	43.30	531.90	153

4. Conclusions

The presented results provide an update of the report on LiDAR based AGB models presented in 2015 for Berau and Kapuas Hulu. Problems with the first iteration of inventory data caused a delay in the processing of the AGB model for Malinau. With the new inventory dataset now available, it was possible to derive a LiDAR based AGB model for Malinau as well.

However, even though the new forest inventory data set is of significantly higher quality than the first dataset, it still has some technical limitations which hamper the creation of a high quality AGB model. First of all, the total amount of forest plots available is not very high. Technical problems or apparent inconsistencies require the exclusion of 11 of the 25 sample plots which leaves only 14 plots for the regression modeling. This number of calibration plots is at the very low end for an AGB regression model.

Furthermore, some of the remaining plots seem to have less than optimal accuracy in geolocation. This inaccuracy can be related to the very steep topography in Malinau, but partly also seems to be caused by errors in the measurement procedure.

As a result of the combination of a low amount of field samples for calibration paired with apparent geolocation problems, the correlation of the field measured AGB with the LiDAR height statistics leads to a regression model with comparably low prediction quality (R^2= 0.49). Therefore, the resulting local AGB values for the different forest types need to be treated with caution. Nevertheless, the model outcomes in terms of average AGB values for the different forest types is considered realistic.